

**SYNTHESIS AND CHARACTERIZATION OF
NANOCOMPOSITE FOR SURFACE ASSIMILATION
OF PHYTOESTROGENS**

A Thesis

**Submitted in the partial fulfillment of the requirement for the
award of the degree of**

MASTER OF SCIENCE

IN

BIOTECHNOLOGY



Under the guidance of:

Dr. Moushumi Ghosh

Associate Professor

Submitted by:

Tania Jurangal

Roll No.301001028

DEPARTMENT OF BIOTECHNOLOGY & ENVIRONMENTAL SCIENCES

THAPAR UNIVERSITY, PATIALA (PUNJAB)-147004

JULY 2012

Certificate

This is to certify that the thesis entitled "Synthesis and characterization of nanocomposite for surface assimilation of phytoestrogens" submitted by Tania Jurangal in partial fulfilment of the requirement for the award of Degree of Masters of Science in Biotechnology to Thapar University, Patiala, is a record of student's own work carried out by her. The report has not been submitted for the award of any other degree or certificate in this or any other University or Institute.



Dr. Moushumi Ghosh
Associate Professor, Supervisor
DBTES, TU
Patiala



Dr M.S.Reddy
Head
DBTES, TU
Patiala



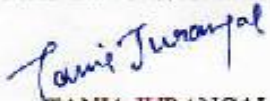
Dr. S.K. Mohapatra
Dean
Academic Affairs,
Thapar University
Patiala

Candidate's Declaration

I, hereby declare that the work which is being presented in the dissertation entitled, "Synthesis and characterization of nanocomposite for surface assimilation of phytoestrogens", in partial fulfillment of the requirement for the award of the degree of Masters of Science in Biotechnology, Department of Biotechnology and Environmental Sciences, Thapar university, Patiala, Punjab; is an authentic record of my own work during a period of six months from January 2012 to July 2012, under the supervision of Dr. Moushumi Ghosh, Associate Professor, Department of Biotechnology and Environmental Sciences, Thapar University. The matter embodied in this thesis has not been submitted in part or full to any other university or institute for the award of any other degree.

Place: Patiala

Date: 16.7.2012


TANIA JURANGAL

Acknowledgement

First and foremost I render my gratitude to the almighty to have conferred blessings on me which has led the path to complete this work successfully. I take this opportunity to thank my esteemed supervisor **Dr. Moushumi Ghosh**, Associate Professor, Department of Biotechnology and Environmental Sciences, Thapar University, Patiala from core of my heart, for her expert guidance, splendid supervision, constant motivation, relentless support, encouragement and inspiration during the course of my dissertation. I consider myself fortunate to have worked under her supervision and thank her once again for her faith in me.

I express my gratitude to **Dr. M. S Reddy**, Head, Department of Biotechnology and Environmental Sciences, Thapar University, Patiala for providing the best laboratory facilities. I owe heartfelt thanks to **Dr. Abhijit Ganguli** for the constant support and guidance throughout the project work.

I am highly thankful for the help rendered by research fellows **Ms. Richu Singla, Ms. Seema Bhanwar, Ms. Gurpreet Kaur Khaira, Ms. Taranpreet kaur and Ms. Gaatha Sharma** throughout my project period without which it would not have been possible for me to achieve my goals. Special thanks to all faculty members and staff, DBTES for their constant encouragement and support throughout the project work.

I feel lacunae of word to express my most heartfelt and cordial thanks to all my friends, who have always been a source of inspiration for me, stood by my side at the toughest times.

I am also thankful to my laboratory staff Mr. Babban and Mrs. Lallita for their help during project work.

Finally, I wish to extend a warm thanks to everybody involved directly or indirectly with my work. Last but not the least, I wish to acknowledge the blessings and immense encouragements of all my elders. No words are enough to describe the overwhelming support and inspiration of my parents and brother.

Date:

TANIA JURANGAL

CONTENTS

Contents	Page No.
Abstract	i
List of Abbreviations	ii
List of Symbols	iii
List of Tables	iv
List of Figures	v-vi
Chapter 1. INTRODUCTION	1-2
Chapter 2. REVIEW OF LITERATURE	3-20
2.1 Phytoestrogens	3
2.2 Chemistry of phytoestrogens	3
2.3 Classification of phytoestrogens	4
2.4 Identification of phytoestrogens	7
2.5 Biological effects of phytoestrogens	8
2.6 Phytoestrogen in industrial wastewater	10
2.7 Phytoestrogens retention & recovery by nanozeolite	11
2.8 Adsorption	18
	21-28
Chapter 3. MATERIALS AND METHODS	
3.1 Synthesis of Nanozeolite	21
3.2 Characterization of nanozeolite	23
3.3 Measurement of phytoestrogen (standard samples)	24
3.4 Optimization studies for maximum reduction and recovery of phytoestrogens	25
3.5 Adsorption capacity	26
3.6 Industrial waste water treatment	27
Chapter 4: RESULTS AND DISCUSSION	29-52
4.1 Synthesis and characterization of Nanozeolite	29

4.2 Determination of wavelength maxima of phytoestrogen	33
4.3 Adsorption dynamics of synthesized zeolite nanocrystals	35
4.4 Detection of phytoestrogen in soy based industrial wastewater	49
SALIENT FINDINGS	53
REFERENCES	54-58

ABSTRACT

Phytoestrogens are diverse group of plant-derived compounds that structurally or functionally mimic mammalian estrogens. The concentrations of Phytoestrogens (1,380 ng/l) are particularly high in wastewater from industries involving soy products. The removal of such hazardous organic compounds from wastewater is one of the most important environmental issues to be solved today. In the present study, the potential usage of nanozeolites as adsorbents for the removal of organic molecules from water was investigated. Two types of nanocrystalline zeolites were synthesized and their size in nanometer range (1×10^{-9} m) was analyzed by characterization (XRD and SEM techniques). The effective adsorption of phytoestrogens (Biochanin A, Formononetin, Coumestrol, Genistein, Daidzein) was optimized i.e. dosage of adsorbent, time of contact between adsorbent and adsorbate. The reduction in phytoestrogens was observed as: Daidzein > Formononetin > Genisetin > Coumestrol > Biochaninn A. The rate of adsorption and selectivity of particular phytoestrogen was analysed using adsorption isotherms of the Langmuir type and calculations showed that the amount of adsorption of phytoestrogen on nanozeolites was significant (60%). The comparative study of two nanocrystalline zeolite estimated that nanocrystalline zeolite Beta was more effective against phytoestrogens.

Keywords: Phytoestrogens, Nanozeolites, Adsorption, Langmuir isotherm

List of Abbreviations

BEA	Zeolite Beta
FAU	Faujasite type zeolite
SiO ₂	Silicon dioxide
Al ₂ O ₃	Aluminum oxide
TEAOH	Tetraethyl ammonium hydroxide
SDA	Structure directing agent
SEM	Scanning electron microscope
XRD	X-ray diffraction
TLC	Thin-layer chromatography
HPLC	High performance liquid chromatography
ER	Estrogen receptor
<i>et al.</i>	Et alteri / et alii (and others)

List of symbols

g	Gram
mg	Miligram
mg/ml	Milligram per mililitre
μg	Microgram
μg/ml	Microgram per mililitre
ng/l	Nanogram per litre
nm	Nanometer (1×10^{-9} m)
%	Percentage
min	Minutes
Å	Angstrom (1×10^{-10} m)
rpm	Revolutions per minute
v/v	Volume by volume
wt%	Weight percent

List of Tables

Tables	Page No.
4.1 Peak list and particle size analysis of nanocrystalline zeolite NaX.	30
4.1(a) Peak list and particle size analysis of nanocrystalline zeolite Beta.	31
4.2(b) Peak list and particle size analysis of commercial nanocrystalline zeolite.	31
4.3 Wavelength maxima of phytoestrogen.	33
4.4(a) Effect of adsorbent dosage (nanocrystalline zeolite NaX).	36
4.4(b) Effect of adsorbent dosage (nanocrystalline zeolite NaX).	36
4.5(a) Effect of treatment time on adsorption by nanocrystalline zeolite NaX.	37
4.5(b) Effect of treatment time on adsorption by nanocrystalline zeolite Beta.	38
4.6 Comparison between different zeolite samples for retention of phytoestrogen.	41
4.7 Shape of isotherm according to RL.	44
4.8(a) Isothermal parameter of phytoestrogen on NaX zeolite.	48
4.8(b) Isothermal parameter of phytoestrogen on Beta zeolite.	49
4.9 R _f value of different spots.	50
4.10 Spectrophotometric analysis of sample.	51
4.11 Retention time (min) and peak area.	53

List of Figures

Figures	Page No.
2.1 The structure of Isoflavones: Biochanin A($R_1=OH, R_2=OCH_3$), Daidzein($R_1=H, R_2=OH$), Formononetin($R_1=H, R_2=OCH_3$), Genistein($R_1=OH, R_2=OH$).	5
2.2 The structure of coumestrol	6
2.3 Illustrates the calculated numbers of atoms on spherical solid nanoparticles (iron) that are surface or bulk (interior) atoms.	13
2.4 A typical synthesis of nanozeolite.	14
2.5 Diffraction scheme	17
4.1 XRD patterns of (a) nanocrystalline zeolite NaX compared with the reference. (b) nanocrystalline zeolite Beta and (c) nanocrystalline commercial zeolite Beta.	30
4.2 The SEM image of (a) nanocrystalline zeolite NaX, (b) nanocrystalline NaX as reference (c) nanocrystalline zeolite Beta and (c) nanocrystalline commercial zeolite Beta.	32
4.3 U.V. scans of phytoestrogen.	34
4.4(a) Effect of adsorbent dosage (nanocrystalline zeolite NaX).	35
4.4(b) Effect of adsorbent dosage (nanocrystalline zeolite Beta).	35
4.5(a) Effect of treatment time on adsorption by nanocrystalline zeolite NaX.	39
4.4(b) Effect of treatment time on adsorption by nanocrystalline zeolite Beta.	40

4.6	Comparison between different zeolite samples for retention of phytoestrogen.	41
4.7	Shape of isotherm according to RL	45
4.8	U.V. scans of phytoestrogen treated by nanozeolite NaX and Beta.	
4.9(a)	Langmuir adsorption isotherm on NaX zeolite (a)Biochanin A,(b)Formononetin,(c)Coumestrol,(d)Genistein ,(e)Daidzein.	46
4.9(b)	Langmuir adsorption isotherm on Beta zeolite (a)Biochanin A, (b) Formononetin, (c)Coumestrol ,(d)Genistein ,(e)Daidzein.	47
4.10	TLC chromatograms of soy sample.	50
4.11	HPLC analysis of standard Daidzein.	51
4.12	Representative chromatogram of soy sample without (a) and with (b) treatment of nanocrystalline zeolite Beta.	52

INTRODUCTION

It is well documented that a large variety of chemical compounds can function as hormone mimics when released into the environment, altering natural endocrine signaling in wildlife. Phytoestrogens, natural plant-derived estrogen mimics, have the ability to disrupt the endocrine system as well. Phytoestrogen exposure has been shown to affect reproductive processes in many different species ranging from mice to fish. In particular, effects on fish are of concern because phytoestrogens may be discharged to surface waters. It has become a source of concern for the public and a subject of intense scientific research. Endocrine disruption occurs when chemical compounds interrupt normal hormonal function in humans and/or wildlife, resulting in infertility, intersex characteristics, and other reproductive and developmental problems. The full extent of the problem is unknown, but scientists agree that endocrine disruption is occurring in wildlife as a result of environmental pollution.

Despite evidence of their estrogenic effects on aquatic organisms, little work has been performed on identifying point sources of phytoestrogens discharge to surface waters. Indeed, only one type of industry, pulp and paper, has been identified as a phytoestrogens point source. Nevertheless, pulp and paper mills are only one of many sources of industrial plant-processing waste. In particular, industries that use soy products are of interest (e.g., biodiesel and soy-based foods), because soy is known to contain the highest levels of phytoestrogens ($1 \times 10^7 \mu\text{g}/\text{kg}$) of any plant. In addition, no work has been conducted on understanding the fate of these compounds in wastewater treatment plants. There is therefore a need to understand both the industrial sources of phytoestrogens and their removal in wastewater processes. This in turn has necessitated the development of new methods for the analysis and quantitative measurement of phytoestrogens. There is a variety of analytical methods in use for phytoestrogens, most offering sensitivity in the low nmol / l range. HPLC with DAD-UV detection is the method of choice and requires minimal sample preparation.

Investigations date back to the 1990s, they covered the removal of pesticides by nanofiltration, which led to the start of several installations on a pilot and industrial scale. At present, reverse osmosis (RO) and nanofiltration (NF), are considered feasible and potential methods of organic

micropollutants removal from water are also taken into account with respect to PhACs (Pharmaceutical Active Compounds) and EDCs (Endocrine Disrupting Compounds) removal.

Reverse osmosis particularly results in lower removal of phytoestrogens than it might be expected. In this case, a need remains for a simple, economical process in which separation of a compound is accompanied by adsorption of micropollutants on and in the structure of the membrane. As adsorption is the process of transferring material from a fluid phase to a solid phase, in which some materials (adsorbate) is concentrated from a bulk vapor or liquid phase on to the surface of a porous solid (adsorbent). So an effective adsorbent is required for this problem.

The most common types of adsorbents for pollution control applications are activated carbons, zeolites (molecular sieves), and synthetic polymers. From economical point of view zeolites are the most suitable adsorbents. They are Host-Guest nanocomposite materials which have high capacity, selective adsorbents that have been widely used for separating a variety of chemical compounds. In host-guest binding weak interactions involve which becomes a reversible process, so that a host and guest can associate and dissociate without either of the building blocks being damaged or altered. Typical examples of zeolite that were useful in the study for retaining phytoestrogen are large pore, hydrophobic zeolite, such as faujasites and beta zeolite, having a high silicon to aluminum ratio. A preferred zeolite adsorbent was zeolite Beta; have a framework structure consisting of 12-member rings with a pore size of about 0.65nm to about 0.75nm. For more effective adsorption, the external surface area was increased by synthesizing nanozeolite which has narrow particle size distribution with sizes of less than 200 nm and act as nanofilters. Adsorption capacities of zeolites were studied using adsorption isotherms and their data were analyzed using Langmuir model.

The focus of the present study was therefore to synthesize potential nanozeolites for comparative study of their reduction towards phytoestrogen and to investigate their applicability in removing phytoestrogens from water of soy based industry.

Objectives

1. Synthesis and characterization of nanocomposite
2. Surface assimilation of phytoestrogen using nanocomposite

REVIEW OF LITERATURE

2.1 Phytoestrogens

Phytoestrogens are plant-derived compounds that structurally or functionally mimic mammalian estrogens and therefore are considered to play an important role in the prevention of cancers, heart disease, menopausal symptoms and osteoporosis (Setchell, 1998). Estrogens influence the growth and functioning of female and male reproductive tissues, maintain the skeletal and central nervous system, provide cardioprotective effects in the cardiovascular system, and protect against colon cancer and aging skin (Gruber *et al.*, 2002).

Phytoestrogens defined functionally are substances that promote estrogenic actions in mammals and structurally are similar to mammalian estrogen 17 β -estradiol (E2). Other mammalian endogenous estrogens are estriol and estrone, which are weakly estrogenic compared with their mammalian counterpart, E2 (Gruber *et al.*, 2002). The diverse biological activity of phytoestrogens is due in part to their ability to act estrogenically as estrogen agonists and anti-estrogenically as antagonists. As estrogen agonists, phytoestrogens mimic endogenous estrogens and cause estrogenic effects. As estrogen antagonists, they may block or alter estrogen receptors (ER) and prevent estrogenic activity, causing anti-estrogenic effects.

Mechanistically phytoestrogens have been shown to bind to two types of estrogen receptors: estrogen receptor α (ER α), which was cloned in 1986, and estrogen receptor β (ER β) cloned in rats and in humans (Mosselman *et al.*, 1996). Phytoestrogens show a lower binding affinity than E2 and some show a higher binding affinity for ER β than for ER α , which may suggest different pathways for their actions and explain tissue-specific variability of phytoestrogenic action (Setchell, 1998). The complexity of phytoestrogens and ERs appears to be further compounded because different transcriptional activities *in vitro* are activated depending on the ligands, as well as the environment of the promoter region of specific genes for translated ER α and ER β receptors. Recent research in teleost fish (Atlantic croaker *Micropogonias undulatus*) identified a third estrogen receptor, ER γ , which is found in various tissues.

2.2 Chemistry of phytoestrogens

There are several classes of phytoestrogens: steroidal estrogens, found in few plants and the more

ubiquitous phenolic estrogens, isoflavones, coumestans and Lignans. Other classes of phytoestrogens that have been reported include: anthraquinones, chalcones, flavones and saponins (Chan *et al.*, 2002). Examples of plant steroids are estrone found in palm (*Elaeis guineensis* Jacq. Areaceae) and β -sitosterol which is found in almost all plants.

Phytoestrogens have been categorized based on their chemical structures, which resemble E2. Estrogen receptors bind with steroidal as well as numerous non-steroidal compounds. An aromatic ring and a hydroxyl group are important for binding effectiveness and the remainder of the ER will accept hydrophobic groups (Anstead *et al.*, 1997). Important features that enable chemicals to bind to an ER are the steric and hydrophobic properties of a compound, as well as the hydrogen bonding between the phenolic hydroxyl group and the ER binding site (Hu and Aizawa., 2003). Estrogenic flavonoids are similar in structure to E2. They are composed of a planar ring system that includes a p-hydroxy-substituted aromatic ring that is approximately 12 Å away from a second in-plane hydroxyl group (Hu and Aizawa., 2003). Two ring structures separated with two carbon atoms as well as spacing between hydrophobic and hydrogen bond interactions are also important in binding affinity to ERs.

Other characteristics for ER-binding affinity of a chemical are the degree and size of branching of the alkyl group and its location on the phenolic ring and the distribution range of electron density on the A ring (Hu and Aizawa., 2003). The biological activity of individual phytoestrogens varies and is often reported as less active than mammal or synthetic estrogens.

2.3 Classification of phytoestrogens

2.3.1 Isoflavones

Isoflavones are the most well known of the phytoestrogens. The recognition of 'clover disease' in Australian sheep in the 1940s led to the investigation of estrogenic activity of isoflavones (Kingsbury, 1964). The sheep whose diet was predominately subterranean clover (*Trifolium subterraneum* L., Fabaceae) suffered from a reproductive disorder that reduced the lambing rates and involved abnormal lactation, changes in the sex organs, permanent infertility, prolapsed uterus and maternal dystocia. Isoflavones are present in green clover and are not present at senescence.

Naturally occurring isoflavones that have shown estrogenic activity are: the aglycones, daidzein (4',7-dihydroxyisoflavone) and genistein (4',5,7-trihydroxyisoflavone); the glycosides, daidzin and genistin; and biochanin A and formononetin, 4'-methyl ethers of daidzein and genistein (Kurzer and Xu, 1997) (Fig.2.1)

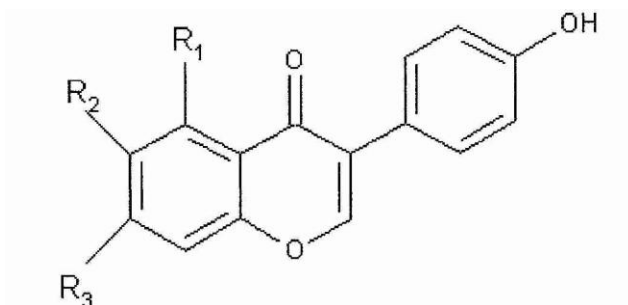


Fig:2.1 The structure of Isoflavones: Biochanin A($R_1 = \text{OH}, R_2 = \text{OCH}_3$), Daidzein($R_1 = \text{H}, R_2 = \text{OH}$), Formononetin($R_1 = \text{H}, R_2 = \text{OCH}_3$), Genistein($R_1 = \text{OH}, R_2 = \text{OH}$).

In plants, they can often be found as glycosides (Ibarreta *et al.*, 2001). In processing, isolation and analysis, these compounds are readily degraded chemically or enzymically to the aglycone. Glycitein is another isoflavone reported in soy that has also shown estrogenic activity. After mammals consume isoflavones, daidzein and genistein are metabolized in the gastrointestinal tract. Biochanin A and formononetin can metabolize to genistein and daidzein respectively. Daidzein may be further metabolized to dihydrodaidzein and then to O-desmethylangolensin (O-DMA) and equol (Kurzer and Xu, 1997). Genistein metabolizes to dihydrogenistein and then to 6'-hydroxy- O-DMA (Kurzer and Xu, 1997) and hormonally inert p-ethylphenol in sheep and humans (Ibarreta *et al.*, 2001).

These new compounds produced from metabolism may have different biological effects than the original isoflavones digested (Naftolin and Stanbury, 2002). Isoflavones are primarily found in the Fabaceae family, which has food legumes such as soy, peanut (*Arachis hypogaea* L.) and clover (*Trifolium* spp.). Soy seeds show high levels of formononetin and biochanin A (Ibarreta *et al.*, 2001). Other food sources of isoflavones are oilseeds and nuts, such as the sunflower seed (*Helianthus* spp., Asteraceae) and walnut (*Juglans nigra* L., Juglandaceae) from different botanical families. Isoflavones have also been found in the Iridaceae and the Euphorbiaceae family.

They are primarily extracted from soy and red clover. Raw soybeans contain 1.2-4.2 mg/g dry weight of isoflavones, while high protein soy ingredients like soy flour contain 1.1-1.4 mg/g dry weight (Kurzer and Xu, 1997).

2.3.2 Coumestans

Coumestans are another group of plant phenols that show estrogenic activity. Coumestrol was first reported in 1957 by Bickoff and coworkers as a new phytoestrogen that was isolated from ladino clover (*Trifolium repens* L., Fabaceae), strawberry clover (*Trifolium fragiferum* L., Fabaceae) and alfalfa or lucerne (*Medicago sativa* L., Fabaceae) (Bickoff *et al.*, 1957). Their presence in fodder crops has been associated with disrupting reproductive performances of livestock. For example, feeding cattle haylage containing 37 ppm (mg/kg) or more of coumestrol resulted in negative estrogenic effects such as udder development, bulling of steers and prolapsed vagina, cervix and rectum (Lookhart, 1980). The main coumestans with phytoestrogenic effects are coumestrol (Fig: 2.2) and 4'-methoxycoumestrol.

Coumestans are less common in the human diet than isoflavones (Ibarreta *et al.*, 2001), yet similar to isoflavones, in that they are also found in legumes, particularly food plants such as sprouts of alfalfa and mung bean (*Vigna radiata* L. R. Wilczek, Fabaceae) (Lookhart, 1980). Soy sprouts also show high levels of coumestrol (Ibarreta *et al.*, 2001).

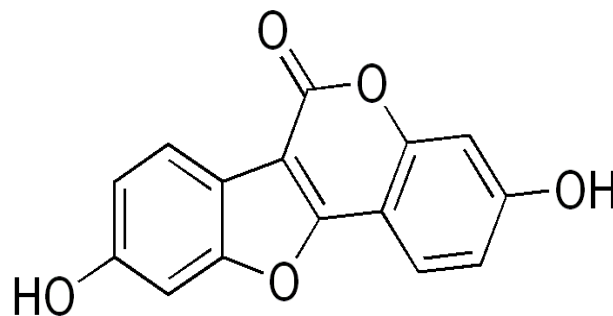


Fig: 2.2 The structure of coumestrol.

2.3.3 Lignans

Lignans were first identified in plants and later in biological fluids of mammals. As a class of compounds they contain a dibenzylbutane skeleton and in plants they aid in the formation of lignin used to construct the plant cell wall (Setchell, 1998). A cyclic pattern observed in the urinary excretion of these phenolic compounds by humans and animals during the menstrual cycle initiated interest in their physiological role. The most well known phytoestrogenic lignans are secoisolariciresinol and matairesinol which are converted by bacterial action in the gut into enterodiols and enterolactone, mammalian lignans not found in plants (Setchell, 1998).

Lignans are widespread in foodstuff such as cereals, fruits and vegetables and have not been studied as thoroughly as isoflavones and coumestans (Ibarreta *et al.*, 2001). Lignans are commonly found in rye bread (*Secale cereale* L., Poaceae) and oilseeds such as flaxseed (*Linum usitatissimum* L., Linaceae). Flaxseed contains the most abundant amount of lignans with about 0.8 mg of secoisolariciresinol/g dry weight (Kurzer and Xu, 1997).

Other compounds that have shown estrogenic activity are: resveratrol (trans-3, 4',5-trihydroxystilbene), diethylstilbestrol (DES) (4,4'-dihydroxy-trans- α,β - diethylstilbene) and mycotoxins such as zearalenol (Bagchi *et al.*, 2001). There is a higher concentration of phytoestrogens in legume plants even though they are also found in grains, vegetables and fruits distributed across the plant kingdom. The most common phytoestrogens found in legumes are isoflavones. Isoflavones are part of the isoflavonoids, which are almost exclusively limited in distribution to the Fabaceae family and more specifically to the sub-family Papilionaceae. Soy or soybean (*Glycine max*) belongs to the Fabaceae family and has long been used as a food plant. Of the bean plants it has one of the highest levels of protein and oil (Duke, 1981). Medicinally it has been reported in ancient Chinese herbals for the healthy functioning of the heart, kidneys, liver and stomach.

2.4 Identification of phytoestrogens

The ability of plant substances to cause estrus in animals was documented in the mid-1920s (Costello and Lynn, 1950). The Allen- Doisy technique was one of the first bioassays to detect estrogenic activity in ovariectomized rats and mice (Allen and Doisy, 1923).

High pressure liquid chromatography (HPLC) was first used to detect flavonoids. It is one of the most common analytical methods used for phytoestrogen identification because limited sample preparation is involved and both glycosides and aglycones can be analyzed directly (Wang *et al.*, 2002). HPLC coupled with a mass spectrometer (LC-MS) is especially useful for this type of analysis. Franke and coworkers (1995) have developed reversed-phase HPLC methods that are tailored for phytoestrogens analysis. Acid hydrolysis is part of sample preparation, which converts glycosides into their respective aglycones. The solvent system they used was a linear gradient of acetonitrile and acetic acid and water with a photodiode array (PDA) detector. This group recently reported a new technique for determining phytoestrogens (Franke *et al.*, 2002). One drawback of using LC-MS is the ineffective isomer differentiation and the inability to produce molecular ions for some flavonoids (Wang *et al.*, 2002).

HPLC coupled with a mass spectrometer (LC-MS) is especially useful for this type of analysis. Franke and coworkers (1995) have developed reversed-phase HPLC methods that are tailored for phytoestrogens analysis. Acid hydrolysis is part of sample preparation, which converts glycosides into their respective aglycones. The solvent system they used was a linear gradient of acetonitrile and acetic acid and water with a photodiode array (PDA) detector. This group recently reported a new technique for determining phytoestrogens (Franke *et al.*, 2002). One drawback of using LC-MS is the ineffective isomer differentiation and the inability to produce molecular ions for some flavonoids (Wang *et al.*, 2002). Additional reports discuss methods used to detect poly-phenolic phytoestrogens in foods and biological fluids. Other non-chromatographic methods have also been used for phytoestrogen analysis, such as immunoassay techniques, deconvolution spectroscopy and matrix-assisted laser desorption ionization time-of-flight mass spectrometry (MALDI-TOF-MS) (Wang *et al.*, 2002).

2.5 Biological effects of phytoestrogens

Investigators have proposed the hypothesis that lowered cardiovascular disease, osteoporotic fractures, rates of breast cancer and hot flushes in Asian populations are related to a diet rich in soy, in other words phytoestrogens. Therefore, diet has been evaluated especially in relation to phytoestrogen content. However, when evaluating this relationship, confounding factors such as

lifestyle, diet, socio-cultural and morphological differences that distinguish Asian and Western populations must be considered in the analysis. Several studies have discussed the potential effects of phytoestrogens in treating breast cancer, endometrial cancer, liver disease and prostate cancer (Fotsis *et al.*, 1993). As studies continue to evaluate the biological effects of phytoestrogens on human health, the complexity is more evident as estrogenic and anti-estrogenic effects are observed as well as a variety of mechanisms of action. Better designed clinical trials are needed to assess the beneficial effects of phytoestrogens on health (Naftolin and Stanbury, 2002).

The mechanisms and potencies of phytoestrogens are not completely clarified and they may be considered potential endocrine disrupters, and therefore caution should be exercised when taking them. The risks associated with phytoestrogens such as increased plasma concentration of isoflavones in babies that ingest soymilk, the ability of non-hormonal secondary plant metabolites to modify sex steroid metabolism, and the effects of phytoestrogens on thyroid (Ibarreta *et al.*, 2001). Several articles have discussed the potential risks involved with soy-based infant formulas (Setchell, 1998). Some negative effects of phytoestrogens may be the result of receiving high levels of isoflavones during fetal development (Setchell, 1998). Studies by showed that infants fed soy-based formula have high concentrations of daidzein and genistein in their plasma, 13 000 to 22 000 times higher than E2 in early life and proportionately higher than normal adult intake of isoflavones.

As potential endocrine disrupters, phytoestrogens may act as antiestrogens and harm the reproductive health of males (Santti *et al.*, 1998). Reduced sperm quality, undescended testes and urogenital tract abnormalities were increased in the sons of mothers taking DES compared with those who did not take the miscarriage preventative drug. Animal studies conducted with DES resulted in male genital abnormalities during development, including cysts, testicular lesions and lack of growth of the seminal vesicles and therefore concern has been raised about the effects of phytoestrogens on male development (Santti *et al.*, 1998). Recent work has shown that prenatal exposure to phytoestrogens may interact with platelet-derived growth factor during testis development. However, Kurzer (1997) reviewed studies on adult men that showed no adverse effects on sperm quality with the consumption of soy isoflavones.

2.6 Phytoestrogen in industrial wastewater

In a recent research, a variety of industries are identified, including biodiesel, soy-oil processing and dairy, that discharged significant amounts of phytoestrogens in their waste. Typically, industries do not discharge their waste (known as effluent) directly into streams and rivers; instead, they discharge their waste to municipal wastewater treatment plants (Lundgren and Novak, 2009). Many researchers have found estrogenic compounds in streams, rivers, and lakes throughout the world, as well as in the effluent of wastewater treatment plants in United States, Europe, Asia, South America, and Australia.

In addition to studies that have shown the widespread and global presence of estrogenic compounds in lakes and rivers, other studies have reported the effects of these compounds on wildlife. For example, many studies have identified abnormal sexual development in fish populations, which has been thought to be a result of exposure to the effluent from nearby wastewater treatment plants. In perhaps the most striking and disturbing study to date, scientists performed a seven year whole lake experiment in northwestern Ontario, Canada, in which very low levels of the active compound in contraceptive pills were added to a lake by the scientists themselves. In addition to observing abnormal sexual development of fathead minnows in the lake, investigators found that the minnows population decreased to near the point of extinction (Kidd *et al.*, 2007). This study clearly demonstrated that whole populations of fish can be at risk from estrogenic pollution, which can produce dramatic ecological effects by altering whole food webs.

As mentioned above, however, industries rarely release their waste directly to streams, rivers, and lakes, but instead send their effluent to local wastewater treatment plant. This process provides an additional layer of protection, because the industrial waste will be further treated. In analysis the inflow and effluent from three wastewater treatment plants, it was found that, In general, elimination of the six target phytoestrogens was high (more than 90%), were removed in all three cases. Unfortunately, in one case a city with a large soy-oil processing facility was unable to reduce the phytoestrogens concentrations to sufficiently low levels, and was releasing environmentally significant levels of phytoestrogens to surface water (1,380 ng/l, or wildlife may occur, which is 1,000ng/l)(Lundgren and Novak, 2009).

An additional point of concern is that some large plant-processing industries are located in small towns, which may use wastewater treatment facilities that are inadequate to sufficiently treat these estrogenic pollutants.

2.7 Phytoestrogens retention & recovery by nanozeolite

Zeolite (Greek, Zeo, “to boil”, lithos, “a stone”) are aluminosilicates that have well defined porous structures. The term was originally coined in the 18th century by a Swedish mineralogist named Axel Fredrik Cronstedt who observed, upon rapidly heating a natural mineral that the stones began to dance about as the water evaporated. Using the Greek words which mean “stone that boils”, he called this material as Zeolite. Zeolites can be described with the following empirical formula $M_{2/n}O \cdot Al_2O_3 \cdot xSiO_2 \cdot yH_2O$, M is cation (Na, Ca, K, Mg & Ba) of valence n, x is ≥ 2 , y is a number determined by porosity & hydration state of zeolite (2-8) (Breck *et al.*, 1974.).

Strictly speaking, zeolites are defined as crystalline microporous aluminosilicates with pore structure consisting of sharing TO_4 tetrahedra, where T is Si or Al. Such tetrahedra are combined in a well-defined repeating structure comprising various combination of 4-, 6-, 8-, and 12-membered rings. The resulting framework structure is a pore network of regular channels and cages that is useful for separation. Zeolites were introduced in 1954 as adsorbents for industrial separations and purifications. Because of their unique porous properties, zeolites are used now in a variety of applications with world production estimated to be in the range of 2.5 million to 3 million metric tons (Mt) in 2008 year. The flexibility of the Zeolite Si-O-Si bond explains the facts that about 200 structures have been determined. More than 150 zeolite types have been synthesized and 48 naturally occurring zeolites are known.

The Atlas of Zeolite Structure Types published by the IZA Structure Commission assigns a three letter code to be used for a known framework topology irrespective of composition. The codes are normally derived from the name of the zeolite or "type material", e. g. LTA for Linde zeolites A, FAU for molecular sieves with a faujasite topology, e.g. zeolites X and Y, MOR for the mordenite topology, MFI for the ZSM-5 and silicate topologies (Kim *et al.*, 2003). The well known and industrially important zeolites have been discovered in 1950-1970 and may be classified into three groups according to Si/Al ratio in their frameworks. "Low-silica" or aluminium rich zeolites A and X (ratio Si/Al ≈ 1), "Intermediate silica" zeolites: zeolite Y, mordenite, zeolite L, natural zeolites

(ratio Si/Al = 2 ÷ 5) "High silica" zeolites: zeolite beta, ZSM-5 (ratio Si/Al ≥ 10).

2.7.1 General properties of zeolites

The presence of Al in the structure of zeolites results in the formation of anion sites within the framework. Charge neutralization may occur by either protonation or by interaction with a metal cation or a hydronium ion. Thus, both Bronsted and Lewis acidities may be present within the zeolite framework. The protonation of the Al-O-Si oxygen center can result in Bronsted acidity in the zeolites structure. Lewis acidity is typically related to the compensating metal ions and defects in the aluminosilicate framework. Bronsted acid sites in zeolites can change into Lewis acid sites through dehydroxylation on heating (Jacobs *et al.*, 1977). The hydrophobicity is an important characteristic of zeolites since it can have a profound influence on their chemical reactivity.

Zeolites containing charges are normally hydrophilic materials that, depending on the framework Si/Ai ratio, can be more or less selective adsorbents for polar or nonpolar molecules. FAU zeolite with the Si/Ai ratio between 2 and 5 is a highly hydrophilic adsorbent. It is then clear that the polarity of a given zeolite could be controlled by controlling the Si/Ai ratio by direct synthesis or by postsynthesis treatments, and this, together with appropriate control of the number of silanol groups by synthesis or postsynthesis treatments should make it possible to prepare zeolite catalysts within a wide range of surface polarities (Corma *et al.*, 2003).

2.7.2 Nanozeolites

Nanozeolites are type of zeolites which have narrow particle size distribution with sizes of less than 200nm (Tosheva *et al.*, 2005). Compared to ordinary zeolites of which the particle diameters are of micrometer order, nanozeolites represent very small particle size, the narrowness of their particle size distributions (often monodisperse) and especially, the fact that they are composed of discrete particles (single crystal) rather than aggregates (Klabunde *et al.*, 1996). The ratio of atoms available on the surface increases as the crystal size decreases (Fig: 2.3). A 20 nm particle has about 10% atoms present on the surface. This feature demonstrates that it is necessary to be very small in order to benefit from the atom economy desired (Klabunde *et al.*, 1996).

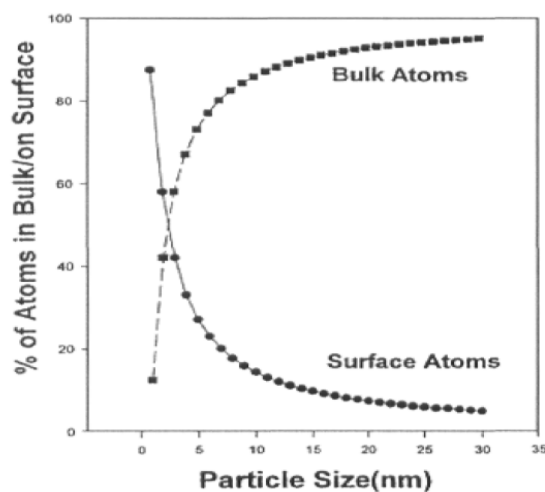


Fig: 2.3 Illustrates the calculated numbers of atoms on spherical solid nanoparticles (iron) that are surface or bulk (interior) atoms.

One of the advantages of nanozeolites is their higher external surface area. The external surface is of vital importance in numerous processes, including adsorption and catalysis. The molecules then diffuse through the micropores of zeolites until they reach active site. Due to the zeolite structure, molecules larger than 7.4 \AA cannot reach active sites located inside the zeolites. This problem can be avoided by replacing the micrometer-sized zeolites with the corresponding nanozeolites. The substitution could lead to a decrease in the diffusional resistance and an increase in the external surface area, hence raising the number of active sites available for large molecules.

Zeolite particles in the 10-100 nm range can bring in new applications of zeolites. The huge surface areas of the nanosized materials dictate that many of the atoms are on the surface, thus allowing good "atom economy" in surface-gas and surface-liquid reactions. Besides the improvement on the external surface areas, nanozeolites have been found to be excellent "building blocks" for constructing structured materials. Hierarchical porous materials with controlled porosity microstructure are of great interest for catalysis and separation applications. The use of preformed zeolite nanocrystals for preparation of supported zeolite films and membranes is one of major applications of nanozeolites. The small size of nanozeolites offers high homogeneity and intactness of the zeolite layer and reduces the number of defects in the film, such as crack and pinholes.

2.7.2.1 Synthesis of Nanozeolite

A number of nanozeolite with different structures has been synthesized such as FAU, MFI, LTA and MOR. Most of them were prepared using clear solutions or gels, however, other methods such as confined space synthesis and synthesis using growth inhibitor have been found to be useful to synthesize these materials. The synthesis of nanozeolite from clear solutions was first discovered by Shoeman *et al.* (1994) and Verduijn *et al.* (1993).

Amorphous reactants containing silica and alumina are mixed together with a structure directing agent (SDA) source, usually in a basic (high pH) medium, resulting in a clear solution. (Fig: 2.4). The aqueous reaction mixture is heated, often (for reaction temperatures around 100 °C) in a sealed autoclave. For some time after rising to synthesis temperature, the reactants remain amorphous. After the above "induction period", crystalline zeolite product can be detected. Gradually, essentially all amorphous material is replaced by an approximately equal mass of zeolite crystals (which are recovered by filtration, washing and drying).

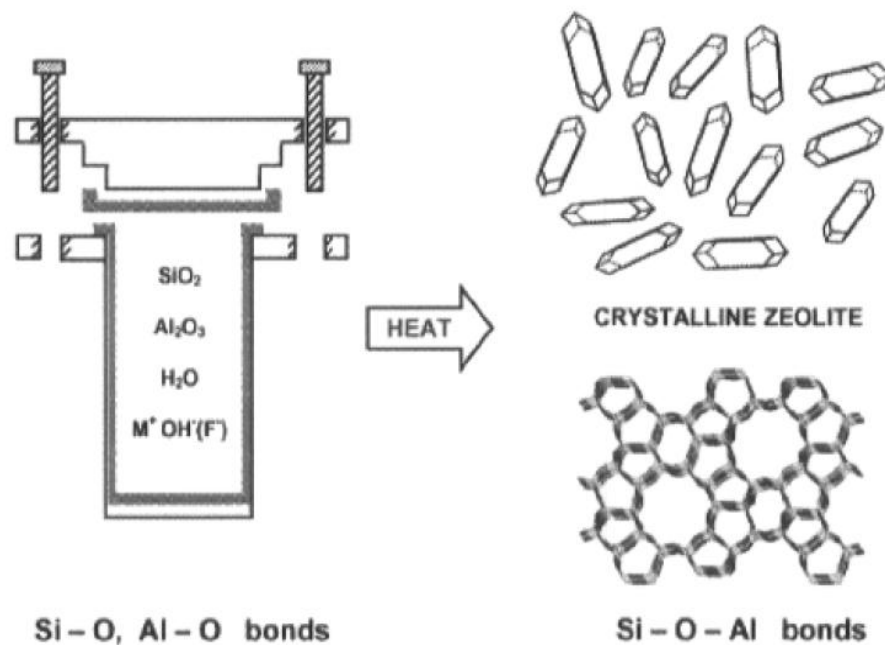


Fig: 2.4 A typical synthesis of nanozeolite.

2.7.2.2 Crystallization Mechanism of nanozeolite from clear solute

Although the crystallization mechanism of zeolite has not been well understood, it has been accepted that the synthesis of nanozeolite in clear solution involves the assembly of very tiny species present in the pre-crystallized solution. For example, in the crystallization of silicalite-1, an all-silica and hydrophobic zeolite, it was revealed that hydrophobic silicates and structure directing agents (SDA) are assembled by hydrophobic interaction, which results in the formation of primary units (ca. 2.8 nm) in the solution prior to nucleation. Subsequently, the nucleation occurs via aggregation of primary units. The primary units are also incorporated directly into the crystalline phase during crystal growth. As a result, nucleation and subsequent crystal growth mechanisms are described by a cluster aggregation scheme. Further study was carried out. (Ravishankar *et al.*, 1998).

In the crystallization of hydrophilic zeolite (low Si/Ai zeolite) using clear solution method, the presence of nanosized amorphous gel particles in the pre-crystallized solution were also found (Mintova *et al.*, 1999). From the TEM observations, (Mintova *et al.*, 1999) revealed that, these amorphous gel particles have different sizes, depending on the starting materials and the zeolite structure. The particles in the synthesis of nanozeolite A were about 5 nm whereas; those in the synthesis of nanozeolite Y were 25-35 nm. The authors proposed that the mechanism involved the aggregation of these particles.

2.7.2.3 Parameters affecting the crystal size

From the perspective of crystallization theory, the crystal size is a function of the ratio between rate of nucleation and rate of growth. Thus, to obtain nanozeolite, one should optimize the following conditions: (i) attaining very high nucleation rates and (ii) providing stabilization of nuclear sized entities. The first condition is controlled by many parameters such as temperature, alkalinity, and aging. The second one depends chiefly on the role of SDAs. Here is a brief review of these parameters.

Temperature: a low crystallization temperature (80 - 100°C) is often applied. This is because temperature raises growth rate more than nucleation rates. However, it should be noted that a too low temperature usually results in poor crystalline, low efficiency, and longer crystallization time.

Aging: the aging of the synthesis mixture at room temperature has significant influence on the nucleation rates. This is due to the fact that nucleation rate is favored at room temperature, but the growth rate is negligible, and thus the nuclei prevail until the temperature is raised.

Alkalinity: the concentration of OH ions strongly increases the solubility of silicate species. In general, smaller zeolite crystals tend to be formed at higher alkalinity. The concentration of the clear solution strongly affects the degree of saturation of the system. At lower supersaturation, growth is favored at the expense of nucleation. Dilution of the solution can cause large crystals to form. Hence a high concentration is a desired parameter. The solubility of the silica source plays an important role in the synthesis of nanozeolite. Smaller crystals are formed from monomeric silicate solutions than by dissolution of colloidal silica. Metal cations usually facilitate the crystal growth. Hence, they should be present in the synthesis solution at low concentration. For example, it has been found that sodium is the growth-limiting nutrient in the formation of Y-type zeolite (Schoeman *et al.*, 1994).

The crystallizations of Y-type and A-type zeolite are very sensitive to sodium content. In some cases, a small variation in this factor results in the formation of a different crystal phase, for the synthesis of zeolite with the clear synthesis gel having molar composition of $2.46 (\text{TMA})_2\text{O} : x \text{Na}_2\text{O} : 1.0 \text{Al}_2\text{O}_3 : 3.40 \text{SiO}_2 : 370 \text{H}_2\text{O} : 13.6 \text{EtOH}$ ($0.03 < x < 0.43$), the sodium concentration of the batch is crucial for controlling which zeolite phase crystallizes. Greater $\text{Na}_2\text{O}/\text{Al}_2\text{O}_3$ ratio (0.43) in the batch favors the formation of zeolite A with a higher yield of 56.5% after a shorter crystallization time. Lower $\text{Na}_2\text{O}/\text{Al}_2\text{O}_3$ ratios (0.03) in the batch produce smaller zeolite Y crystals with a lower yield of 8.1% after a longer crystallization time.

Structure directing agent (SDA): SDAs are often quaternary of the type $[\text{R}_4\text{N}]^+ \text{OH}^-$ (where R is an alkyl group, typically CH_3 , C_2H_5 , C_3H_7 or C_4H_9). The presence of SDA in the synthesis solution helps assist the formation of a desired zeolite structure. Furthermore, SDA is responsible to the stabilization of silicate sub colloidal particles as well as the nanozeolite.

2.7.3 Characterization

X-ray Diffraction (XRD) is a technique in crystallography in which the pattern produced by the diffraction of X-rays through the closely spaced lattice of atoms in a crystal is recorded and then analyzed to reveal the nature of that lattice. XRD is a powerful technique for determining zeolite crystal structure (Fig: 2.5).

Moreover, sample preparation is relatively easy, and the test itself is often rapid and non-destructive

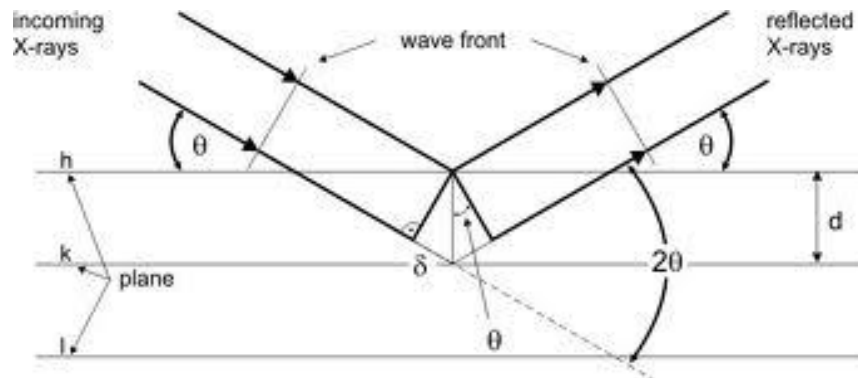


Fig: 2.5 Diffraction scheme

The mechanism of XRD was well explained by Bragg in 1913 (Koningsveld *et al.*, 1999). A crystal can be considered to be composed of discrete parallel planes or layers of atoms. As the wave enters the crystal, it will be partially reflected by the first layer of atoms, while the rest of it will continue through to the second layer, where the process continues. The separately reflected waves will remain in phase if the difference in the path length of each wave ($2d\sin\theta$) is equal to an integer multiple of the wavelength ($n\lambda$).

$$2d\sin\theta = n\lambda$$

This equation is known as Bragg's law, where:

- n is an integer,
- λ is the wavelength of x-rays, and moving electrons, protons and neutrons,
- d is the spacing between the planes in the atomic lattice, and
- θ is the angle between the incident ray and the scattering planes.

Waves that satisfy this condition interfere constructively and result in a reflected wave of significant intensity, causing a peak in the pattern diffraction.

The pattern of powder diffraction peaks can be used to quickly identify materials (thanks to the zeolite pattern database (Baerlocher *et al.*,2001) and changes in peak width or position can be used to determine crystal size and crystallinity (Baerlocher *et al.*,2001) of zeolites. The crystallinity of zeolite can be derived from XRD as follows:

$$\text{Crystallinity (\%)} = \text{Intensity of peak sample at } 2\theta = 22.48^\circ / \text{Intensity of peak reference at } 2\theta = 22.48^\circ \times 100$$

The reference sample is assumed to be 100% crystalline.

The crystal size, a is calculated according to Scherer's equation:

$$r = k\lambda/\beta\cos\theta$$

Where k is the shape factor, λ is the x-ray wavelength, typically 1.54 Å, β is the line broadening at half the maximum intensity (FWHM) in radians, and θ is the Bragg angle.

However, the largest crystals contribute more to the average size determined by XRD than the small crystals. Hence, crystal sizes determined from XRD of very small zeolite crystals are not very accurate and should be taken as first approximations to the true crystal size. In a typical test, a zeolite sample was characterized by powder wide-angle XRD, recorded on a Siemens D5000 X-ray diffractometer using CuK_α radiation ($k = 1.54184 \text{ \AA}$). The samples were scanned over a range of 2 θ values from 5 to 50° with a scan step size of 0.02° and a scan step time of 1s.

Scanning electron microscope (SEM) is a microscope that uses electrons rather than light to form an image. As the primary electron beam "scans" across the sample, the electrons on the surface of the sample are excited. This excitation leads to the emission of the secondary electron beam from the surface which produces the image. The SEM can produce images of high resolution, which means that closely spaced features can be examined at a high magnification. Images obtained from this technique can provide information about the surface and particle size of the samples. Preparation of the samples is relatively easy since most SEMs only require the sample to be conductive.

2.8 Adsorption

Adsorption process is among most economic and feasible methods which can be applied as an in situ or a "pump and treat" option. Activated carbon has been the most widely used adsorbent so far; however, due to its high costs of preparation and reactivation, there have been great efforts to replace

it with new adsorbents, which are economically viable and more compatible to the environment (Bowman, 2003).

Zeolites are a well known aluminosilicate family of inorganic adsorbents, which have an infinite, open, and rigid three-dimensional structure. The three-dimensional framework of zeolites consists of $(\text{AlO}_4)^{5-}$ and $(\text{SiO}_4)^{4-}$ tetrahedral units linked through shared oxygen atoms, which cause overall negative structural charges resulting a high cation exchange capacity (Breck 1974). Surface modification of zeolites by means of cationic surfactants can lead to suitable adsorbents for anionic species (e.g., chromates, nitrates, etc.) and organic contaminants among such as BTEX compounds.

Clinoptilolite is the most abundant natural zeolite which is found vastly in huge resources worldwide and has a high chemical and mechanical strength which makes it a promising candidate for preparation of natural zeolite nanoparticles by mechanical grinding and milling (Charkhi *et al.* 2010). Milling and size reduction of zeolite particles to nanosized range increases the available surface area and decreases diffusion path length and as a result it would increase the adsorption efficiency (Charkhi *et al.* 2010). Size reduction of zeolite particles by grinding and milling normally takes place by means of wet and dry ball milling in order to prevent the destruction crystalline structure. One of the options for using nanoparticles as water treatment media is granulation of nanoparticles with a glue-like media and consequently removal of this binder media, usually by calcination at higher temperature. This process is really rapid and particle size control, handling, and modification of the adsorbents are easily possible.

The urge of implementing nanotechnology in environmental friendly applications is obvious in order to develop and introduction of new inorganic-based adsorbents as potential substitutions of activated carbon. It can be anticipated that these new adsorbents based on porous zeolitic nanoparticles can be considered as a promising inexpensive adsorbents. Different adsorption mechanisms may be found by studying the dependence of adsorption on various variables (pH, concentration of solutes, ionic strengths, and the type and topology of surfaces), and by interpreting the parameters of the determined adsorption isotherms. Also, thermodynamic parameters of adsorption from solutions provide a great deal of information concerning the type and mechanism of the adsorption process.

2.8.1 Adsorption Isotherm equations and thermodynamic parameters

There are several types of adsorption from solutions isotherms (Giles *et al.*, 1974). Langmuir and Freundlich isotherms are the most commonly used models, since they can be applied to a wide range of adsorbate concentrations. The general form of the Langmuir equation for adsorption from solution is:

$$Q_e = Q_{\max} \frac{K_L C_e}{1 + K_L C_e}$$

where q_e is the amount of adsorbate adsorbed on the adsorbent at equilibrium (mol g^{-1}), q_{\max} is the maximum adsorption capacity corresponding to a complete monolayer coverage on the adsorbent surface (mol g^{-1}), K_L is the Langmuir constant ($\text{dm}^3 \text{mol}^{-1}$), and c_e is the concentration of adsorbate at equilibrium (mol dm^{-3}). The values of q_{\max} and K_L can be evaluated from the slope and the intercept of the linear form of the Langmuir equation:

$$C_e/Q_e = 1/Q_{\max} K_L + C_e/Q_{\max}$$

The characteristics of Langmuir isotherm is defined by a dimensionless constant called separation factor or equilibrium parameter, R_L , which was defined by (Weber *et al.*, 1974):

$$R_L = 1/(1 + k_L c_0)$$

The parameter R_L indicates the shape of isotherm.

MATERIALS AND METHODS

Zeolites are obtained as natural minerals as well as can be synthesized. The synthetic ones are widely used as adsorbents, catalysts and ion-exchange materials. For phytoestrogen adsorption, particular nanozeolites are required which can be more effective adsorbent. The nanozeolites were synthesized and their effectiveness was studied using various parameters.

3.1 Synthesis of Nanozeolite

The mechanism of zeolite formation are very complex due to the plethora of chemical reactions, equilibrium and solubility variations that occur throughout the heterogeneous synthesis mixture during the crystallization process. For phytoestrogen recovery, useful zeolites are FAU-type and BEA-type of zeolite

The FAU-type zeolite includes X- and Y-types, Si/Al ratios of which are 1-1.5 and 1.5-3.0, respectively.

3.1.1 Synthesis of Nanosized NaX Zeolite (Mahdi *et al.*, 2011)**3.1.1.1 Reagents and materials**

The chemical reagents such as fumed silica (7 nm) and sodium aluminate solution (NaAlO₂) were purchased from Sigma Aldrich. Sodium hydroxide (pellets) was purchased from SDFCL. 250 ml plastic bottle and deionized water was used for zeolite synthesis.

The nanometer-sized faujasite-X zeolite was synthesized by hydrothermal crystallization in a temperature-controlled shaker. An aluminosilicate gel containing 5.34 g of NaOH, 2.42 g of NaAlO₂, 3.43 g of SiO₂, and 50.0 g of H₂O was adopted. First, a 250-mL plastic bottle containing freshly prepared sodium aluminate solution and fumed silica, the silicate sources were directly mixed with freshly prepared aluminate solution at room temperature and then immediately moved to a shaker at 60 °C for 4 days in a shaker with a rotation rate of 250 rpm for hydrothermal crystallization. The powdered products were recovered with centrifugation, washed with DI water until pH < 8, and then dried at room temperature for 24 h for further characterization.

Zeolite Beta (IZA code, BEA) was first synthesized by Zeolite beta represents the first high silica zeolite (Si/Al = 10-100) synthesized from a gel with alkali metal and an organic template, tetraethyl ammonium cations. BEA can be described by the general formula: $\text{Na}_n [\text{Al}_n\text{Si}_{64-n}\text{O}_{128}]$, where $n = 7$. The first clues to the crystal structure of zeolite beta were evident from chemical and physical property measurements. BEA contains at least 12 membered-ring channels (Higgins *et al.*, 1988). Zeolite beta has pore diameters of 0.76 x 0.64 nm and 0.55 x 0.55 nm. The BEA framework topology attracts much attention because of the large available pore. The complete exchange of cations is possible in BEA as the presence of channels instead of cages compare with FAU-type zeolite.

3.1.2 Synthesis of nano-crystalline zeolite beta (Modhera *et al.*, 2008)

LUDOX AS-40 Colloidal Silica (40 wt%) and Tetra-Ethyl Ammonium Hydroxide (TEAOH, 35 wt% in water), Aluminium Sulphate and Sodium Hydroxide (Pellets).

The molar compositions: $1\text{SiO}_2:x\text{Al}_2\text{O}_3:6.29\text{TEAOH}:0.154\text{Na}_2\text{O}$, where $x = 0.02$ for Si/Al molar ratio 25 and 0.005 for Si/Al molar ratio 100. Colloidal Silica of 3.27 g was added to a mixture of comprising of 5.49 g aqueous solution of TEAOH and 0.2693 g NaOH pellets with vigorous stirring for 30 minute to form a clear gel. An aqueous solution containing x g $\text{Al}_2(\text{SO}_4)_3$ (where $x = 0.2745$ g for Si/Al molar ratio 25 and 0.0686 g for Si/Al molar ratio 100) was added to the mixture. Ethanol formed during hydrolysis was evaporated resulting into a viscous gel, which was aged under stirring at room temperature for 24 h. Hydrothermal treatment of nucleated gel was carried out in a stainless steel autoclave with Teflon cup (75 mL) for 48 h at various crystallization temperatures 80 °C to 180°C under autogenous pressure with rotation condition. The resulting solid product was filtered and washed with de-ionized water until the pH of filtrate less than 9 was observed. The solid was dried at 110 °C for 10 h.

3.2 Characterization of nanozeolite

3.2.1 X-ray Diffraction

Crystal size and crystalline phase purity of the synthesized samples were determined by X-ray powder diffractometer (XPRT-PRO). Zeolite materials, being crystalline solids have characteristic diffraction patterns that can be used to identify their exact structure and to determine their degree of Crystallinity. The diffractions of X-rays from zeolite crystallites produce a scattering pattern which is specific of the periodic arrangement of regular arrays of atoms or ions located within the zeolite structure. Each zeolite has its own specific XRD pattern that can be used as reference for the solid crystal phase and as a fingerprint for the zeolite. This technique can also signify whether the solid sample is amorphous or crystalline. The purity of the solid crystal can be measured by comparing the XRD pattern of the sample with the XRD pattern of the standard sample. The determination of the degree of Crystallinity is based on the intensity of the characteristic peaks at around $2\theta = 22.5^\circ$ (d302). The degree of Crystallinity calculated after background correction, is taken as the peak intensity of the zeolite sample divided by the peak intensity of the parent zeolite material that is taken as reference for 100% Crystallinity. The degree of Crystallinity is calculated using the following formula:

$$\text{Crystallinity (\%)} = \text{Intensity of peak sample at } 2\theta = 22.48^\circ / \text{Intensity of peak reference at } 2\theta = 22.48^\circ \times 100$$

The reference sample is assumed to be 100% crystalline.

The crystal size, is calculated according to Scherer's equation:

$$r = k\lambda/\beta\cos\theta$$

Where k is the shape factor, λ is the x-ray wavelength, typically 1.54 Å, β is the line broadening at half the maximum intensity (FWHM) in radians, and θ is the Bragg angle.

The XRD patterns for NaX and Beta nanozeolite were recorded using Cu radiation (40 mA, 45 kV) over a two-theta angular range of 5.0016-39.9846 at 0.0130/18.8700s and 5.0084-79.9784 at 0.0170/25.1973 respectively. The measured diffraction patterns were interpreted by using the PDF Database sets 1-52, Jade6.0 and CSM search/match software.

3.2.2 Scanning Electron Microscope (SEM)

Scanning electron microscope (SEM) is a microscope that uses electrons rather than light to form an image. As the primary electron beam "scans" across the sample, the electrons on the surface of the sample are excited. This excitation leads to the emission of the secondary electron beam from the surface which produces the image. The SEM can produce images of high resolution, which means that closely spaced features can be examined at a high magnification.

The crystal morphology was examined with a scanning electron microscope (SEM-5000), with resolution 6.0nm (Tungsten filament) and having an EDS detector. The samples were coated with gold using a Polaron Sputter Coater. The nanozeolite samples were coated with gold and their crystal morphology was analyzed under different magnifications.

3.3 Measurement of phytoestrogen (standard samples)

3.3.1 High Performance Liquid Chromatography (HPLC)

The phytoestrogen (standard samples) ie Biochanin A, Formononetin, Coumestrol, Genistein, Daidzein were purchased from Sigma Aldrich.

HPLC has proven to be the method of choice since the 1980s. Generally, phytoestrogens can be separated with mixtures of methanol, acetonitrile and aqueous acids or buffers as modifiers using reversed-phase C-18 stationary matrices. In the latest review on the measurement of food flavonoids (Merken and Beecher, 2000) point to the diverse and ever-increasing use of HPLC in analysis of phytoestrogens. A HPLC method was developed for phytoestrogens to achieve baseline separation using standards.

The analyses was performed using a Reverse phase column NovaPak-C-18(150mmx 3.9mm x 4µm). A Shimadzu LC-10 AT VP HPLC system with SPD 10 A VP UV-VS Detector was used. Column temperature was maintained at 30 °C. Samples were injected individually through a syringe filter. Elution was performed at 0.8mL/min with the following stepwise gradient. Where A =acetonitrile, B =acetic acid-water (10:90;v/v), 30% A in B (v/v) ran for 20 minutes; from 20 minutes to 35 minutes, B changes from 70% to 30%, finally A ran for 25 minutes. The samples were detected by UV absorbance. All solvents used for HPLC and optical density readings were of analytical or HPLC grade (Franke *et al.*, 1995).

3.3.2 Determination of wavelength maxima

Phytoestrogens have distinct ultraviolet (UV) absorption spectra; it is therefore possible to enhance detection selectivity using detector wavelengths at 260 and 280 nm, as well as to provide a positive confirmation of identity. The spectrum of phytoestrogen consists of two absorption maxima in the ranges 245 to 275 and 300 to 330 nm, with low relative intensities in the latter range. The UV absorption spectra of daidzein, formononetin, and genistein in methanol (λ_{\max}) are 238sh, 249, 260sh, 303sh; 240sh, 248, 259sh, 311; and 261, 328sh nm, respectively. The concentration of stock solutions of Phytoestrogens can be determined by absorbance readings at the wavelength with maximum absorption (λ_{\max}) using molar extinction coefficients (ϵ) after proper dilution with methanol using the following values: daidzein ($\lambda_{\max}= 250 \text{ nm}, \epsilon= 20,893$), genistein ($\lambda_{\max}= 263 \text{ nm}, \epsilon= 37,154$), formononetin ($\lambda_{\max}= 256 \text{ nm}, \epsilon= 29,512$), biochanin A ($\lambda_{\max}= 263 \text{ nm}, \epsilon= 27,542$), and coumestrol ($\lambda_{\max}= 339, \epsilon= 22,330$) (Franke *et al.*, 1994). Absorption spectra of the isoflavones daidzein, genistein, formononetin, and biochanin A in water show strong absorption between 250 and 270 nm and a rather weak band or shoulder in the 300- to 350-nm region. Coumestrol has maxima at 240 and 355 nm (Beekman *et al.*, 1999).

For the study of wavelength maxima of phytoestrogens, U.V spectrophotometer-TOSHVIN (A11454907898 analytical) was used. The concentration of prepared stock solutions of phytoestrogen in methanol was determined and λ_{\max} values were used to compare treated samples.

3.4 Optimization studies for maximum reduction of phytoestrogen

3.4.1 Optimization of Nanozeolite dose

To study the effect of synthesized nanozeolite dose, experiments were run using three different concentrations of nanocrystalline (NaX and Beta) i.e. 0.25mg, 0.5mg, 1mg and 1.5mg. Nanozeolite doses (0.25mg/ml-1mg/ml) were added to the phytoestrogens (standard solution) and vortexed for 30 seconds and shake manually for maximum time to facilitate adsorption, then the mixture was spin (spinwin) at 10,000 rpm for 1 minute, to separate liquid and solid phases. The nanozeolite sample was settled down and the supernatant was collected and its absorbance was measured. To analyze the efficiency of the nanozeolite dose, the reduction in the initial and final

absorbance of the

phytoestrogen was estimated. Each experiment was performed in triplicate. Observations were made discussed in results and discussion.

3.4.2 Optimization of Time of contact

The contact time optimization experiment was conducted to obtain how long the adsorbent would take to absorb maximum amount of phytoestrogens. 1mg of each of the modified adsorbents was weighed and phytoestrogens (standard solution) were added to the adsorbent. The contact time ranges was set from 1min–10 min for every sample as above this time constant absorbance was observed. Vortexing was performed for every sample of about 30seconds and then simply shaken for respective time. Then, the mixture was spin (spinwin) at 10,000 rpm for 1minute, to separate liquid and solid phases. Each experiment was performed in triplicate. The UV-vis absorption of the sample was checked and analyzed.

3.4.3 Phytoestrogen retention

The phytoestrogen retention by nanozeolite was estimated by simply measuring the absorbance of the sample. The optimized dose of nanozeolite was taken (1mg) and phytoestrogens were treated for the optimized contact time (1-6min) for the maximum adsorption. The intial and final value was measured and the maximum percentage retention by nanozeolites was calculated. Each experiment was performed in triplicate.

3.5 Adsorption capacity

Adsorption capacity of the zeolite at equilibrium (Q_e , mg/g) was calculated by using the following equation:

$$Q_e = (C_oV_o - C_eV_e)/m$$

Where C_o and C_e are initial and final sample concentrations ($\mu\text{g/ml}$) respectively, V_o and V_e are the initial and final volume of the sample solution and m is the weight of adsorbent added.

3.5.1. Adsorption isotherms

The Langmuir isotherm model uses the following linear form equation:

$$C_e/Q_e = 1/Q_{\max} K_L + C_e/Q_{\max}$$

Where Q_e is adsorption capacity at equilibrium (mg/g), Q_{\max} is the maximum adsorption capacity (mg/g), C_e ($\mu\text{g/ml}$) is the solution concentration at equilibrium, and K_L is the Langmuir constant (l/mg). Separation factor or equilibrium parameter, R_L , which was defined by (Weber and Chakkravorti, 1974):

$$R_L = 1/(1 + K_L C_0)$$

The parameter R_L indicates the shape of isotherm.

3.6 Industrial waste water treatment

In Comparison to other industrial plant-processing waste the concentrations of phytoestrogens is particularly high in wastewater from industries manufacturing soy products (e.g., biodiesel refining, soy oil production, and soy milk processing). Soy is known to contain the highest levels of phytoestrogens ($1 \times 10^7 \mu\text{g/kg}$) (Liggins J. *et al.*, 2000). For the study, of reduction of phytoestrogen from industrial waste water which act as point source of phytoestrogen discharge to surface waters the sample was collected from soy based waste water industry.

3.6.1 Collection of sample

The soy industrial waste water sample was collected from Garcha pure products farm, sangrur near Patiala. 100ml of the waste water containing soy manufacturing waste was evaporated completely to 10ml. Then, scrapped and dissolved in methanol for further analysis.

3.6.2 Qualitative and quantitative analysis of phytoestrogen presence in wastewater sample

3.6.2.1 Thin layer chromatography (Beck (1964))

Thin-layer chromatography (TLC) has been used in the identification of isoflavonoids. Precoated polyamide 6 TLC plates have been used for the initial fractionation of isoflavones and phenolics from soybeans and soy products (Pratt and Birac, 1979). The methanolic extracts are spotted on 20×20 cm plates and developed using methanol–acetic acid–water (90:5:5).

Bands are eluted with methanol and rechromatographed on polyamide using chloroform–methanol–methyl ethyl ketone(12:2:1). For aglycones, the plates are developed in ethyl acetone–petroleum ether(3:1) and then in ethanol–chloroform (1:1). Bands are detected with appropriatechromogenic sprays or with a UV lamp at 366 nm. Diethylether extract chromatographed on a silica plate developed three times in dichlo-romethane–methanol (95:5, v/v) gave the following Rf: daidzein, 0.20; genistein,0.30; formononetin, 0.55; and biochanin A, 0.75, respectively.

The method used for the TLC analysis of the sample was given by Beck (1964). Phytoestrogen standard solutions (as reference) and soy industrial waste water sample in methanol (0.5µg/ml) were used, and the development was carried out in a solvent system of chloroform/methanol (89: 11, v/v) on silica gel plates. Detection was carried out directly at UV-254 nm after exposure to fumes of concentrated ammonia solution.

3.6.2.2 High Performance Liquid Chromatography (HPLC) determination of phytoestrogen in waste water sample (Franke *et al.*, 1995)

HPLC analyses was performed using a Reverse phase column NovaPak-C-18(150mmx 3.9mm x 4µm). A shimadzen LC-10 AT VP HPLC system with SPD 10 A VP UV-VS Detector was used. Colum temperature was maintained at 30 C. Samples were injected individually through a syringe filter. Elution was performed at 0.8mL/min with the following stepwise gradient. Where A =acetonitrile, B =acetic acid-water (10:90;v/v), 30% A in B (v/v) ran for 20 minutes; from 20 minutes to 35 minutes, B changes from 70% to 30%, finally A ran for 25 minutes. The samples were detected by UV absorbance. All solvents used for HPLC and optical density readings were of analytical or HPLC grade. The chromatogram of soy sample was observed .Observations was made discussed in results and discussion.

RESULTS AND DISCUSSION

In the present study, nanozeolites were synthesized for the study of retention of phytoestrogen. These phytoestrogens are endocrine disruptors and they are present in industrial waste water, which is of prime concern. Here, the potential of nanozeolites for treatment of industrial waste water was investigated and the efficacy of interaction between nanozeolites and phytoestrogen was studied with respect to adsorption process.

4.1 Synthesis and characterization of Nanozeolite

Temperature controlling and agitation processes in the synthesis of nanoparticles are important. Increase in temperature and agitation promote the synthesis of nanozeolite with small crystals of nanometer range (1×10^{-9} m). It is well known that synthesis time directly affect the crystallization process. The NaX nanocrystal product was obtained after 4-days crystallization while Zeolite Beta was obtained within 1-2 days crystallization. Higher product yield and bigger particle size was obtained at longer synthesis time. In the study these factors i.e. temperature, agitation and time were taken into consideration and nanozeolite were synthesized. The total product obtained of nanozeolite NaX and Beta were 0.66 g and 1.499 g, respectively.

4.1.1 X-ray Diffraction

The diffractions of X-rays from zeolite crystallites produce a scattering pattern which is specific of the periodic arrangement of regular arrays of atoms or ions located within the zeolite structure. Each zeolite has its own specific XRD pattern that can be used as reference for the solid crystal phase and as a fingerprint for the zeolite. XRD is important for concluding crystal size, crystalline phase purity and measurement of solid sample amorphous or crystalline nature.

The XRD pattern of the nanocrystalline zeolite NaX synthesized are shown in Fig: 4.1(a). The XRD pattern of the nanocrystalline zeolite NaX is identical to that of the reference, indicating the FAU structure of the sample. There is a clear broadening of the reflections from the sample and the decrease in peak intensity, which is attributed to the presence of small crystals.

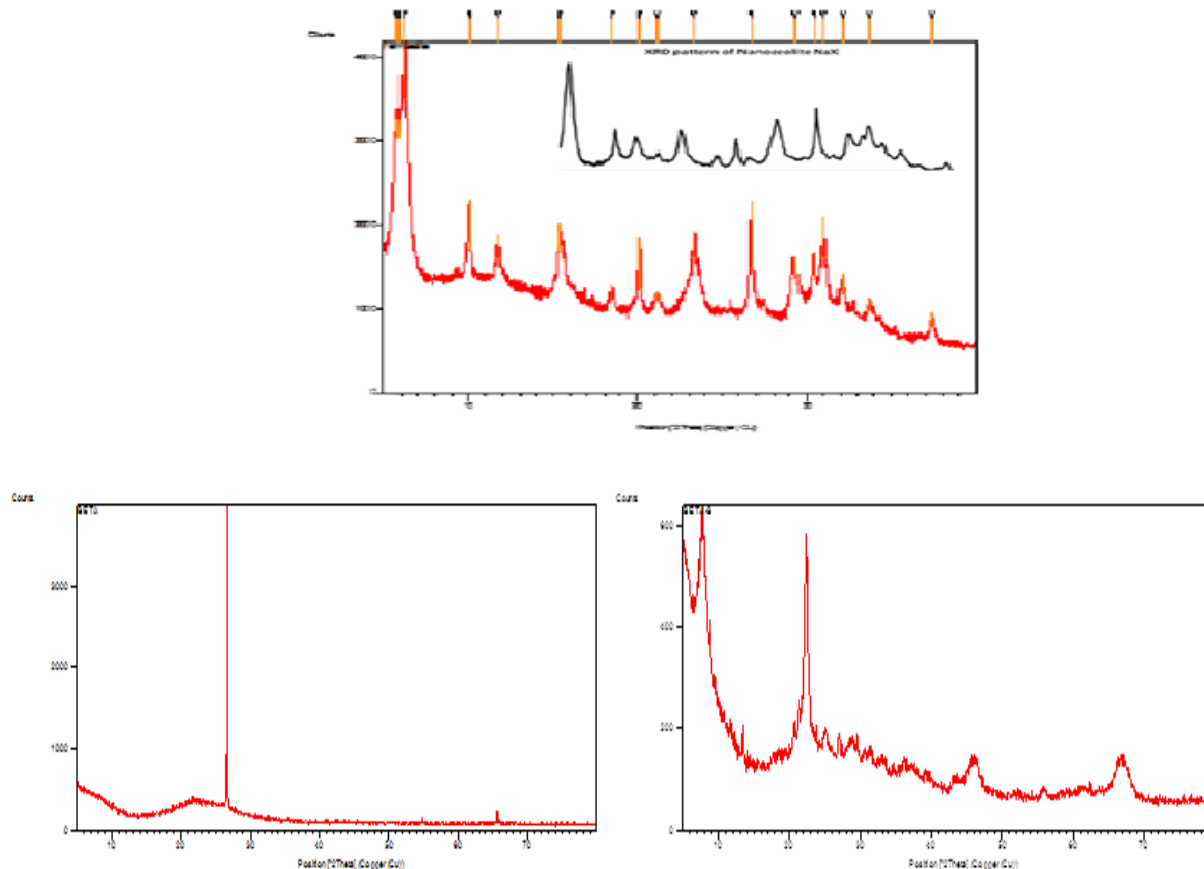


Fig: 4.1 XRD patterns of (a) nanocrystalline zeolite NaX compared with the reference. (b) nanocrystalline zeolite Beta and (c) nanocrystalline commercial zeolite Beta.

The XRD pattern of the as synthesized nanocrystalline zeolite Beta with Si/Al ratio of 25 as shown in Figure: 1(b) sharp and broad reflections of peaks were observed and is identical to that of commercial nanocrystalline zeolite Beta (Fig: 1(c)).

Peak	θ (Pos.)	β (FWHM)	Particle size (nm)
1.	9.223	0.1791	88
2.	11.66	0.1535	104
3.	13.36	0.1407	114
4.	14.67	0.2303	114
5.	15.51	0.1535	105.4

Table 4.1 Peak list and particle size analysis of nanocrystalline zeolite NaX.

Peak	θ (Pos.)	β (FWHM)	Particle size (nm)	Peak	θ (Pos.)	β (FWHM)	Particle size (nm)
1.	13.28	0.0669	23.69	1.	4.416	0.1004	15.4
2.	17.67	0.4015	4	2.	6.708	0.1171	13.27
3.	27.35	0.0816	20.8	3.	10.301	0.2007	7.81
4.	32.815	0.0612	29.05	4.	15.71	0.4015	7.89

Table 4.2 Peak list and particle size analysis of (a) nanocrystalline zeolite Beta, (b) commercial nanocrystalline zeolite.

The average crystal dimension of 105.08 nm was calculated by Scherrer's equation for nanocrystalline zeolite NaX. The average crystal dimension for nanocrystalline zeolite Beta and commercial nanocrystalline zeolite Beta was 19.3 nm and 11.3 nm, respectively. This proves that the synthesized nanocrystalline Beta product was in nanometer range and is similar with commercial nanocrystalline Beta.

The determination of the degree of crystallinity is based on the intensity of the characteristic peaks at around $2\theta = 22.5^\circ$ (d302). The degree of crystallinity calculated after background correction, is taken as the peak intensity of the zeolite sample divided by the peak intensity of the parent zeolite material that is taken as reference for 100% crystallinity. The degree of crystallinity is calculated using the following formula:

$$\text{Crystallinity (\%)} = \text{Intensity of peak sample at } 2\theta = 22.48^\circ / \text{Intensity of peak reference at } 2\theta = 22.48^\circ \times 100$$

The reference sample is assumed to be 100% crystalline.

The degree of Crystallinity, calculated was 71% for nanocrystalline zeolite NaX and 100% for nanocrystalline zeolite Beta.

4.1.2 Scanning Electron Microscopic analysis (SEM)

The morphology and crystal size was examined by SEM.

As shown in Fig: 4.2 images of nanocrystalline NaX and zeolite Beta obtained after synthesis, was compared with that of their respective commercial standard. These images clearly indicate the size of nanozeolites was ultrafine and the morphology of synthesized nanozeolites was found to be spherical.

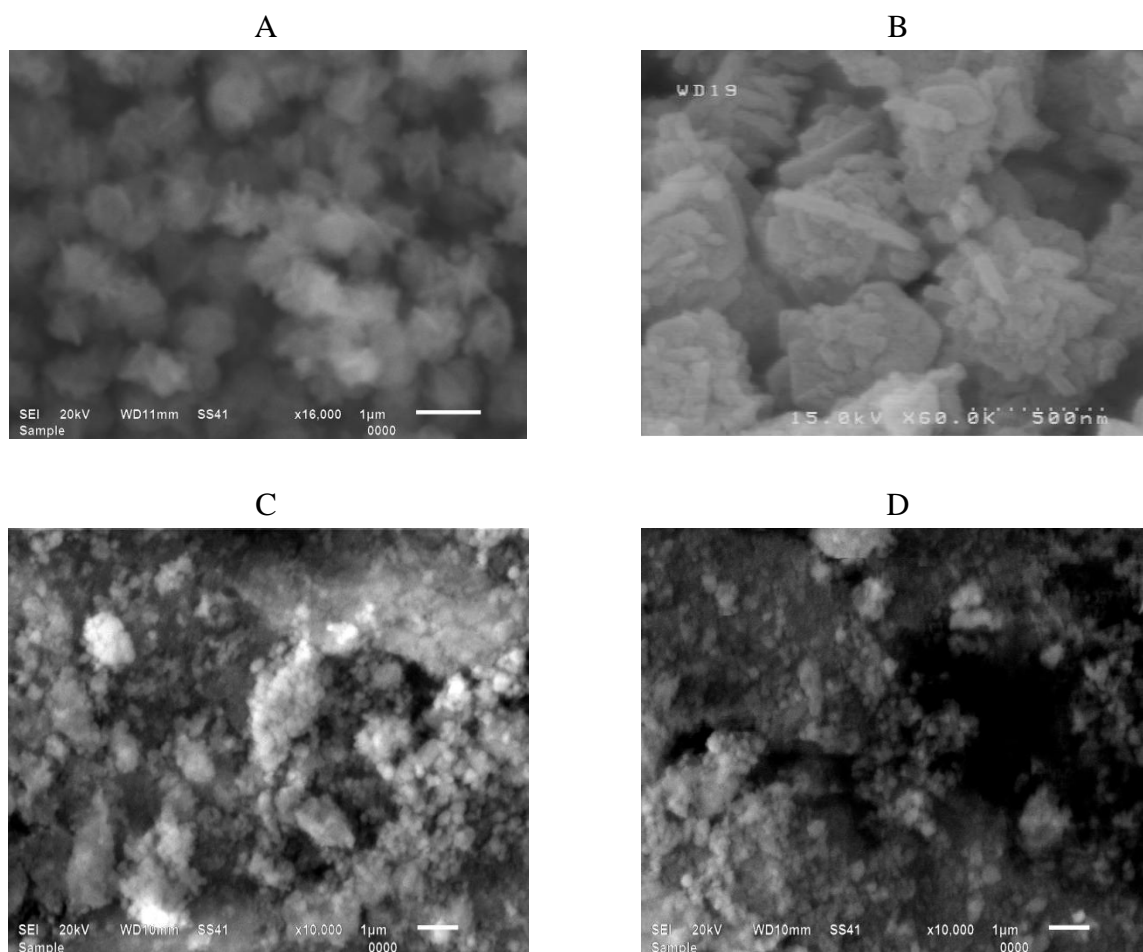


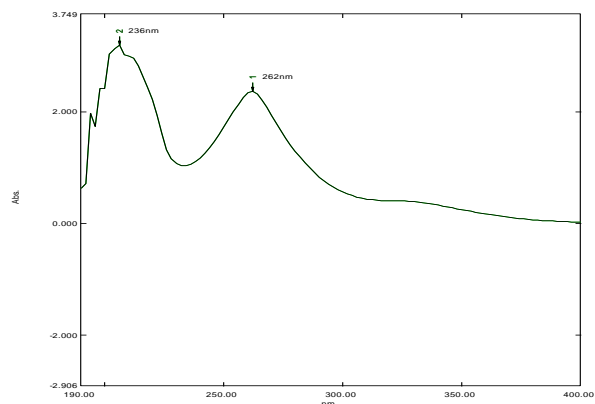
Fig: 4.2 The SEM image of (A) nanocrystalline zeolite NaX, (B) nanocrystalline NaX as reference (C) nanocrystalline zeolite Beta and (D) nanocrystalline commercial zeolite Beta.

4.2 Determination of wavelength maxima of phytoestrogen

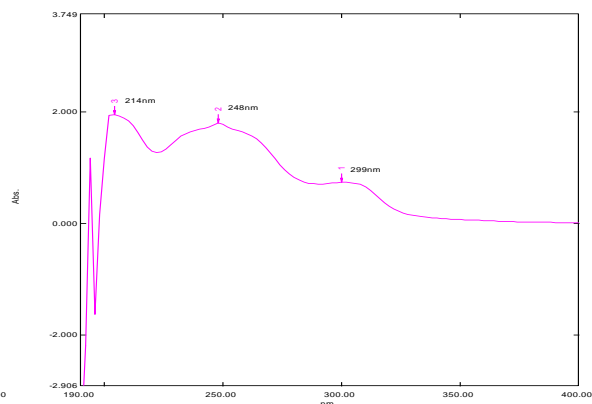
Phytoestrogens have distinct ultraviolet (UV) absorption spectra. This is useful in the study as it enhance detection selectivity. The UV absorption spectra of daidzein, formononetin, and genistein in methanol (λ max) are 238sh, 249, 260sh, 303sh; 240sh, 248, 259sh, 311; and 261, 328sh nm, respectively. The the wavelength with maximum absorption (λ max) using molar extinction coefficients (ϵ) after proper dilution with methanol using the following values: daidzein (λ max= 250 nm, ϵ = 20,893),genistein (λ max= 263 nm, ϵ = 37,154), formononetin (λ max= 256 nm, ϵ = 29,512),biochanin A (λ max= 263 nm, ϵ = 27,542),and coumestrol (λ max= 226, ϵ = 22,330) was describe by Franke *et al.*,(1994). The study of wavelength maxima of phytoestrogens was measured by U.V. Scan (Table 4.3),(Fig:4.3).

Table:4.3 Wavelength maxima of phytoestrogen.

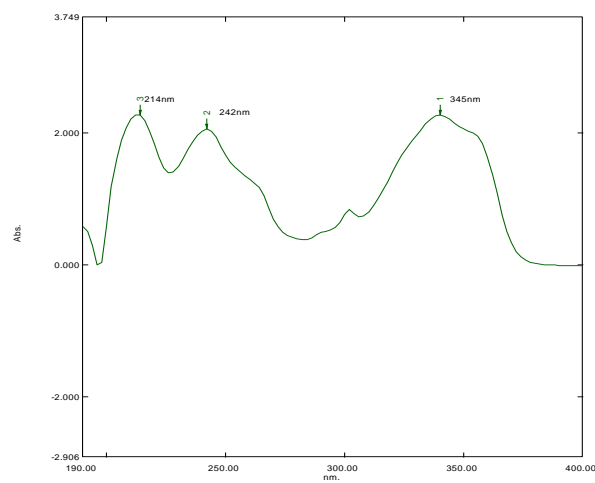
Phytoestrogen	λmax (nm) (methanol)
Biochanin A	236,262
Formononetin	248,299
Coumestrol	214,242
Genistein	260,330
Daidzein	232,300



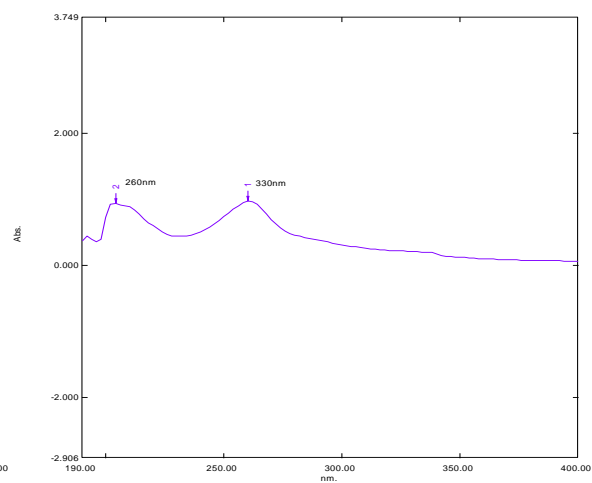
Biochanin A



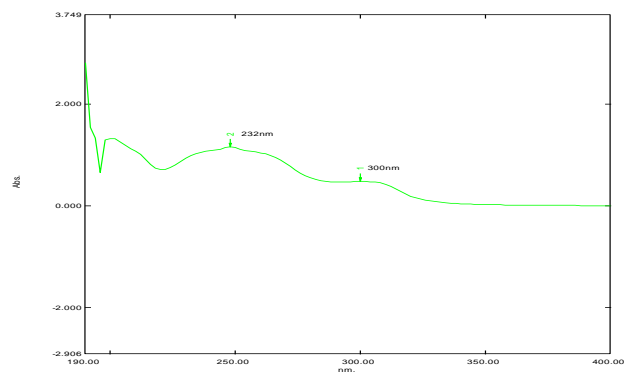
Formononetin



Coumestrol



Genistein



Daidzein

Fig:4.3 U.V. scans of phytoestrogen.

4.3 Adsorption dynamics of synthesized zeolite nanocrystals

4.3.1 Dose optimization

The synthesized NaX and Beta nanocomposites were used as adsorbents. Optimization of their dosage is one of the most important parameter in determining the optimum condition for the adsorption process. The series of experiments were run to determine the optimum adsorbent dosage. The study was carried out by taking the adsorbent range from 0.25mg/ml-1.5 mg/ml for both the nanocrystalline zeolites, NaX and Beta. The time range was considered in the dose optimization experiment was 1-20 mintues. Further time was optimized.(Fig:4.4(a) and (b)).

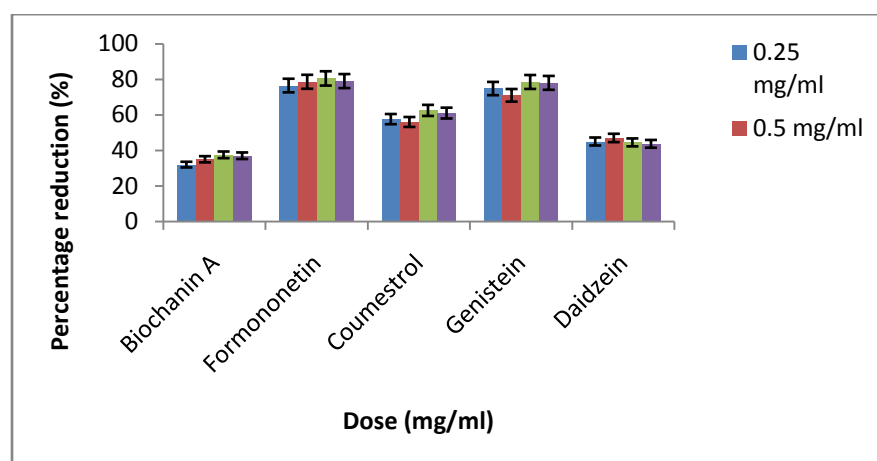


Fig:4.4(a) Effect of adsorbent dosage (nanocrystalline zeolite NaX).

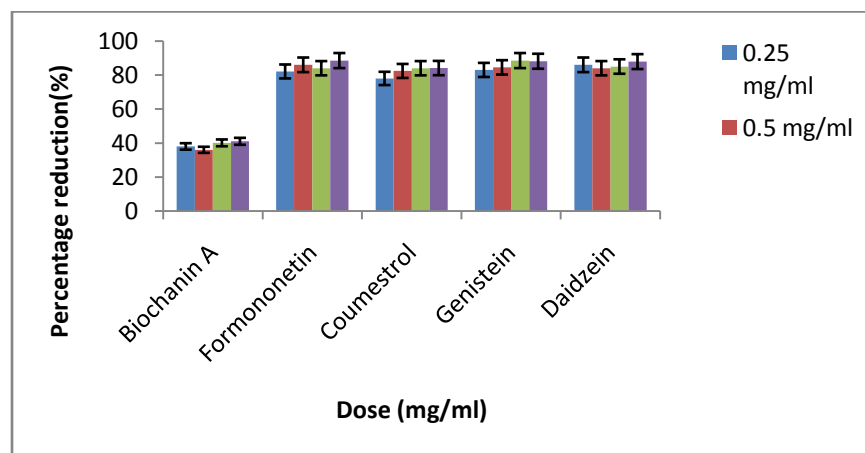


Fig:4.4(b) Effect of adsorbent dosage (nanocrystalline zeolite Beta).

It was observed that at adsorbent dosage of 0.25 mg to 1.5mg and at concentration of 1µg/ml phytoestrogens, there is increase in adsorption when phytoestrogens were treated with a dosage of 1mg/ml. The reduction percentage of phytoestrogen was increasing with increase in dose of the adsorbent. The reduction in the level of the phytoestrogens used was observed to be the same in both nanocrystalline zeolite NaX and Beta (adsorbents). Overall, nanocrystalline zeolite Beta had the maximum ability as compared to NaX. (Table:4.4(a),(b)).

Table 4.4(a) Effect of adsorbent dosage (nanocrystalline zeolite NaX).

Dose (mg/ml)	Percentage reduction by nanocrystalline zeolite NaX (%)				
	BiochaninA	Formononetin	Coumestrol	Genistein	Daidzein
0.25	35±0.7	76.5±0.2	57.6±0.1	74.8±0.4	45±0.2
0.5	35±0.1	78.6±0.4	56±0.8	71±.08	47±0.4
1	37.5±0.3	80.5±0.8	62.5±0.4	78.5±0.3	44.5±0.1
1.5	37±0.2	79±0.3	61±0.5	78±0.2	43.7±0.3

Values are mean ± standard deviation

Table 4.4(b) Effect of adsorbent dosage (nanocrystalline zeolite Beta).

Dose (mg/ml)	Percentage reduction by nanocrystalline zeolite Beta (%)				
	BiochaninA	Formononetin	Coumestrol	Genistein	Daidzein
0.25	38±0.1	82.1±0.6	78±0.5	83±0.8	86±0.4
0.5	36±0.2	86±0.3	82.4±0.4	84.5±.04	84±0.2
1	40.1±0.2	84±0.1	84±0.1	88.5±0.2	85±0.1
1.5	41±0.3	88.5±0.4	84.1±0.3	88.1±0.4	87.9±0.5

Values are mean ± standard deviation

From the above study it was concluded that with increasing adsorbent dosage more active sites were available, making phytoestrogen penetration to the adsorption sites easier and increasing the adsorption capacity. The adsorption of phytoestrogen remained almost constant at adsorbent dosage higher than 1mg/ml. 1mg/ml was selected as optimum concentration for adsorption as with increasing concentration almost same adsorption was observed this might be due to the saturation i.e. all the active sites are occupied by the phytoestrogen and no further adsorption can occur (Ruthven *et al.*, 1988). Therefore, the optimum dose of adsorbent (nanocrystalline zeolite NaX and Beta) used for further studies was 1 mg/ml.

4.3.2 Effect of contact time

Besides the effect of adsorbent dosage, the contact of time also play crucial role in adsorption process for reduction in phytoestrogens. As the adsorption process requires proper contact between the adsorbent and adsorbate. Hence, vortexing (30sec) was done followed by shaking to increase the effectiveness of the process. It was observed that optimum adsorption of all the phytoestrogens were achieved within the first 2-6 minutes and remained fairly stable thereafter (Fig:4.5 (a),(b)). The percentage reduction of phytoestrogen with time was observed with both nanocrystalline zeolite NaX and nanocrystalline zeolite Beta and it analyzed that nanocrystalline zeolite Beta is more efficient in reduction of phytoestrogen compare to nanocrystalline zeolite NaX. The reduction percentage of Daidzein was maximum by nanocrystalline zeolite Beta (89.5%) while percentage reduction of Formononetin was maximum by nanocrystalline zeolite NaX (84.5%) as shown in table: 4.5 (a) and (b).

Table:4.5(a) Effect of treatment time on adsorption by nanocrystalline zeolite NaX.

Time (minutes)	Percentage reduction by nanocrystalline zeolite NaX (%)				
	BiochaninA	Formononetin	Coumestrol	Genistein	Daidzein
2	35.5±0.3	72±0.2	57.6±0.2	76.05±0.4	41±0.2
4	36.7±0.1	74±0.6	67±0.4	80±0.05	45±0.1
6	42.25±0.1	84.5±0.05	65±0.1	83.35±0.3	44.55±0.05
8	41.25±0.2	80±0.4	61.75±0.05	79.1±0.1	44.15±0.1
10	39.99±0.4	77.75±0.4	61.95±0.05	79±0.05	42.5±0.05

Values are mean ± standard deviation

Table:4.5 (b) Effect of treatment time on adsorption by nanocrystalline zeolite Beta.

Time (minutes)	Percentage reduction by Beta nanozeolite (%)				
	BiochaninA	Formononetin	Coumestrol	Genistein	Daidzein
2	38.9±0.4	84.5±0.1	82.55±0.2	83±0.2	80.9±0.2
4	41.5±0.6	88.55±0.1	83.5±0.1	88±0.1	83±0.3
6	43.05±0.4	87±0.05	86.5±0.1	85.95±0.1	89.5±0.1
8	41±0.5	86.4±0.01	84.5±0.05	84.6±0.1	86±0.3
10	39.5±0.4	84.25±0.1	83±0.1	84.15±0.05	85.5±0.5

Values are mean ± standard deviation

When zeolites are in contact with phytoestrogen, the adsorption process takes place. Adsorption occurs in a series of three steps. In the first step, the chemical compound is transferred from the liquid phase to the external surface of the adsorbent material. In the second step, the chemical compound diffuses from the relatively small area of the external surface into the macropores, transitional pores, and micropores (or nanopores) within each adsorbent. Most adsorption occurs in the micropores (or nanopores) because the majority of available surface area is there. In the third step, the chemical compound adsorbs to the surface in the pore. Steps 1 and 2 occur because of the concentration difference between the liquid phase passing through the adsorbent and near the surface of the adsorbent. Step 3 is the actual physical bonding between the molecule and the adsorbent surface. This step normally occurs more rapidly than steps 1 and 2. (Turk A. *et al.*, 1977).

Therefore, with increase in time of contact the adsorption of the chemical compound start increasing and when the highest level of adsorption occurs the saturation point was there as the result further adsorption was not possible because the pores in the adsorbent surface are occupied by the chemical compound.

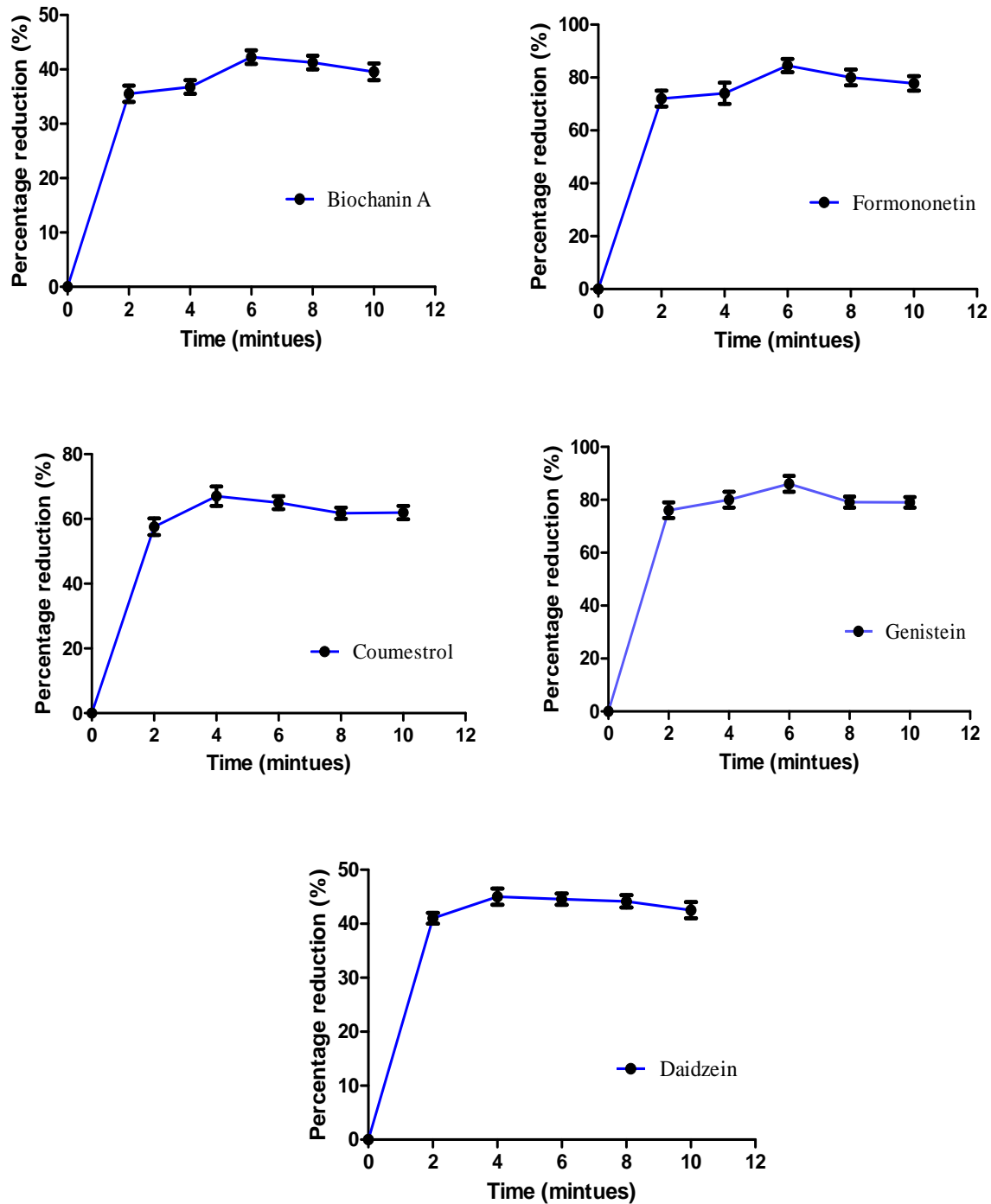


Fig :4.5 (a) Effect of treatment time on adsorption by nanocrystalline zeolite NaX.

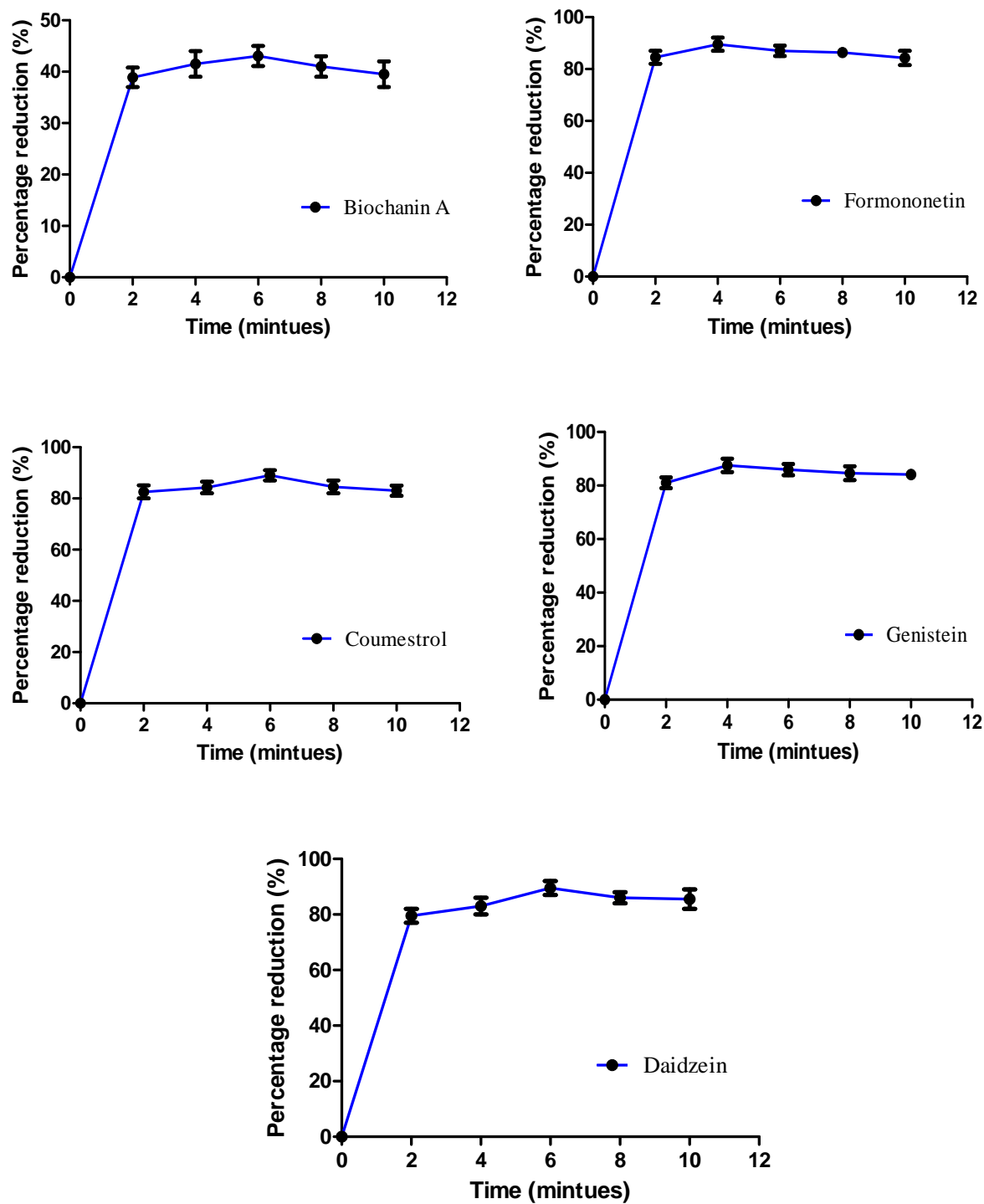


Fig :4.5 (b) Effect of treatment time on adsorption by nanocrystalline zeolite Beta.

4.3.3 Percentage retention of phytoestrogens using nanozeolite

Two different nanozeolites, nanocrystalline zeolite NaX and nanocrystalline zeolite Beta were used to study the effectiveness of adsorption of phytoestrogen. It was observed that nanocrystalline zeolite Beta was more efficient and has high retention capacity compare to nanocrystalline zeolite NaX as shown in Table (4.6). The trend in retention by nanocrystalline zeolite NaX and Beta of phytoestrogen is in order of Formononetin > Genistein > Coumestrol > Daidzein > Biochanin A and Daidzein > Formononetin > Genistein > Coumestrol > Biochanin A respectively(Fig:4.6).

Table :4.6 Comparison between different zeolite samples for retention of phytoestrogen.

Phytoestrogen($\mu\text{g/ml}$)	Percentage retention (%)	
	NaX zeolite	Beta zeolite
Biochanin A	42.25 \pm 0.1	43.05 \pm 0.4
Formononetin	84.5 \pm 0.05	88.55 \pm 0.1
Coumestrol	67 \pm 0.4	86.5 \pm 0.1
Genistein	83.35 \pm 0.3	88 \pm 0.1
Daidzein	45 \pm 0.1	89.5 \pm 0.1

Values are mean \pm standard deviation

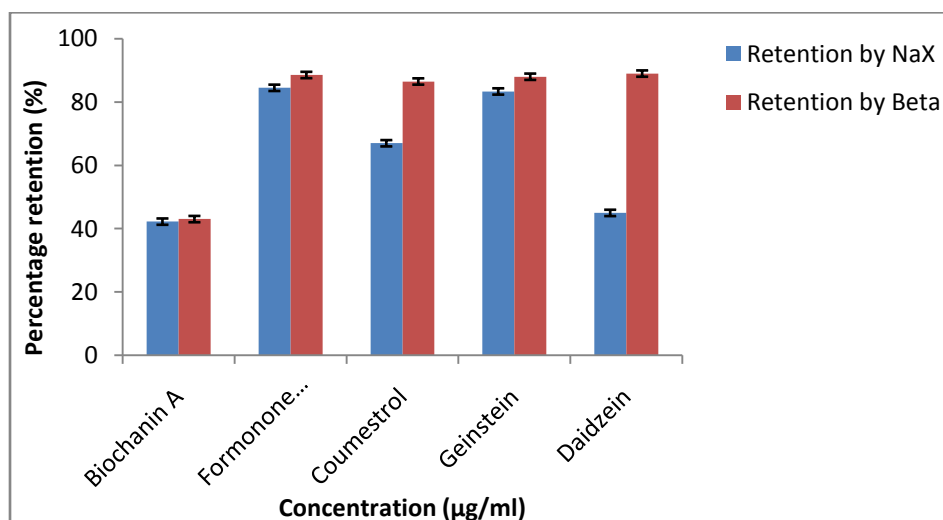


Fig: 4.6 Comparison between different zeolite samples for retention of phytoestrogen.

Due to the uniformity of the pore dimensions, zeolites can act as "host materials" for many molecules. Only molecules of certain size are able to adsorbed by a given zeolite material, or pass through its pores, while molecules of bigger size cannot. In the study particle size reduction of zeolite to the nanometer scale leads to substantial changes in the properties of zeolite which make them promising materials for adsorption.

The nanocrystalline zeolite NaX and Beta has three dimensional cage or channel systems, and may discriminate competing molecules on the basis of the difference in their molecular shape (Bowen T.C *et al.*, 2004). The adsorption of Daidzein is maximum among phytoestrogen by nanocrystalline zeolite Beta. The molecular weight of Daidzein is lowest i.e (254) compare to other phytoestrogens (Biochanin A (284), Formononetin (268), Coumestrol (272.4), Genistein (270). The phytoestrogens were dissolved in methanol for the adsorption process and the kinetic diameter of alcohols (methanol, ethanol, isopropanol and n-butanol) used in the study are smaller than the smallest pores of zeolite beta, which is 5.6 Å. (Tamer, 2006). Therefore, they can fill in the pores of the zeolite Beta, to a great extent and almost at the same amount.

The interaction between nanozeolites and phytoestrogen is a physical process and the forces active in physical adsorption are electrostatic in nature and occur under suitable conditions. These forces are present in all states of matter: gas, liquid, and solid. Physical adsorption is also referred to as Vander Waals adsorption. Because of Vander Waals forces, physical adsorption can form multiple layers of adsorbate molecules, one on top of another. The electrostatic effect that produces Vander Waals forces depends on the polarity of both the liquid and solid molecules. Phytoestrogen have log pK_w of around 2 which proves their moderate hydrophobicity and polar in nature. In this case, separation of a compound is accompanied by adsorption. The aluminium in the zeolite tends to make the zeolite hydrophilic. With increasing silica content and decreasing aluminium, the zeolite becomes more hydrophobic and therefore the greater the ability of these materials to interact with hydrophobic organic molecules or to exclude hydrophilic molecules, such as water. The transition from hydrophilic to hydrophobic occurs at about SiO₂/Al₂O₃ = 20. Nanocrystalline zeolite Beta is more hydrophobic compare to nanocrystalline zeolite NaX as the the Si/Al ratio (Si/Al = 25-100) is high compare to nanocrystalline zeolite NaX. Nanocrystalline zeolite Beta is better adsorbent as more active sites become available and also as there are no steric restrictions and more of phytoestrogen

will adsorbed on its surface (Breck D.W *et al.*, 1964).The localized electrostatic poles between the positively charged cations and the negatively charged zeolite framework strongly attract highly polar molecules.

4.3.4 Determination of wavelength maxima of phytoestrogen treated with nanocrystalline zeolite NaX and Beta

The U.V. scan of the phytoestrogen treated with nanocrystalline zeolites was studied. The reduction in peaks was observed (Fig: 4.8).

4.3.5 Adsorption capacity

Adsorption capacity of the zeolite at equilibrium (Q_e , mg/g) was calculated by using the following equation:

$$Q_e = (C_oV_o - C_eV_e)/m$$

Where C_o and C_e are initial and final sample concentrations ($\mu\text{g/ml}$) respectively, V_o and V_e are the initial and final volume of the sample solution and m is the weight of adsorbent added.

The linear form of Langmuir isotherm equation is given as:

$$Q_e = Q_{\max} K_l C_e / 1 + K_l C_e$$

Where C_e (mg/ml) is the equilibrium concentration of the adsorbate, Q_e (mg/g) is the amount of adsorbate adsorbed per unit mass of adsorbent, Q_{\max} and K_l are Langmuir constants related to maximum adsorption capacity and rate of adsorption, respectively.

The plot of C_e/Q_e vs. C_e , is a straight line with slope of $1/q_m$ and intercept of $1/Q_{max}Kl$ (Fig: 4.9(a)and (b)).

The characteristics of Langmuir isotherm is defined by a dimensionless constant called separation factor or equilibrium parameter, R_L :

$$R_L = 1 / (1 + KIC_0)$$

The parameter R_L indicates the shape of isotherm and it can be clearly seen from the shape of the adsorption isotherm that it belongs to Langmuir type of adsorption as shown in Table:4.7.

Table 4.7 : Shape of isotherm according to R_L .

R_L	Isotherm
$R_L > 1$	Unfavorable
$R_L = 1$	Linear
$0 < R_L < 1$	Favorable
$R_L = 0$	Irreversible

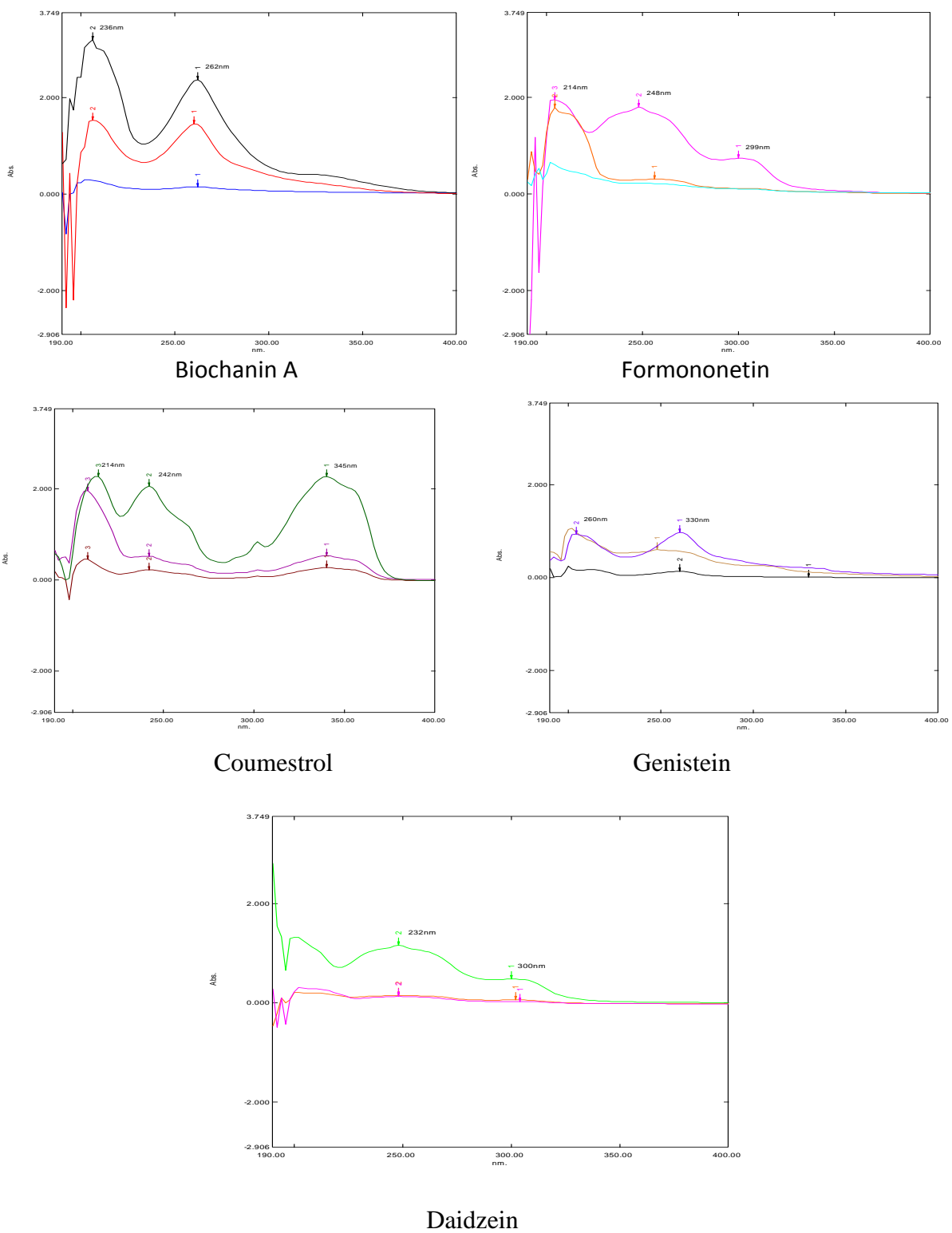


Fig: 4.8 U.V. scans of phytoestrogen treated by nanozeolite NaX and Beta

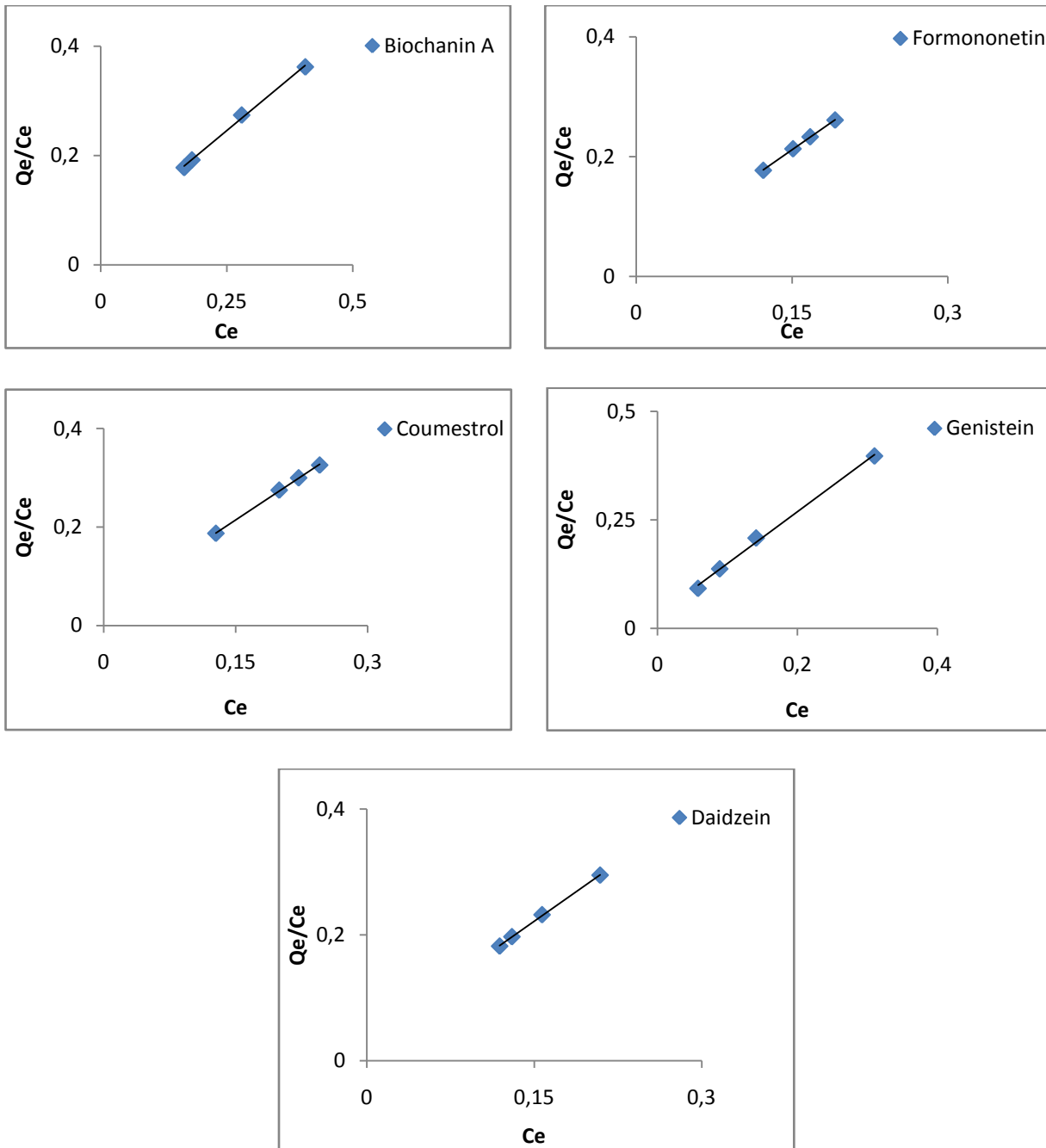


Fig:4.9 (a) Langmuir adsorption isotherm on NaX zeolite (a)Biochanin A, (b)Formononetin, (c)Coumestrol ,(d)Genistein ,(e)Daidzein.

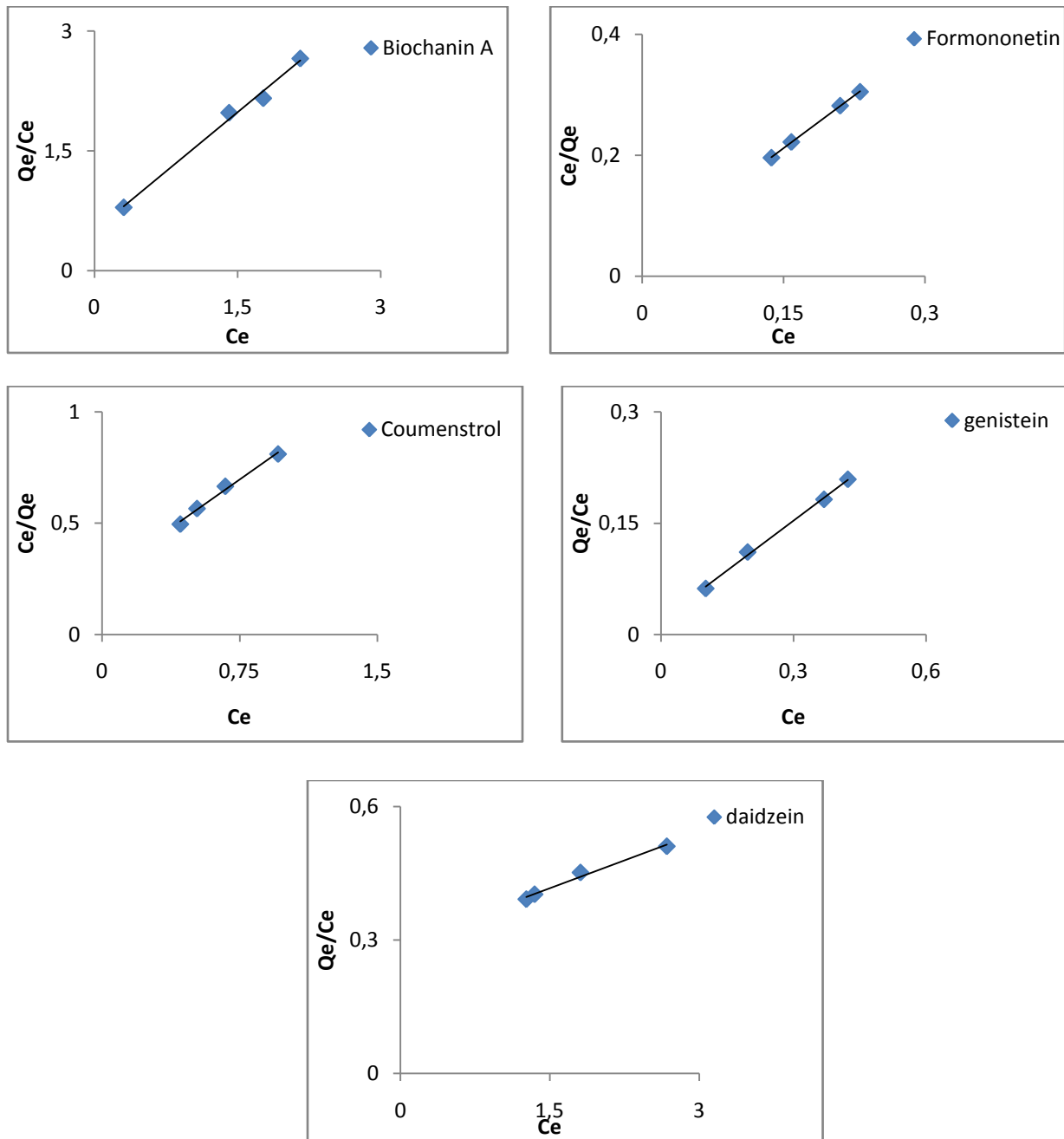


Fig:4.9(b) Langmuir adsorption isotherm on Beta zeolite (a)Biochanin A, (b)Formononetin, (c)Coumenstrol, (d)Genistein, (e)Daidzein.

The Q_{max} and KL are the parameters involve in measurement of the adsorption process. KL is a constant related to the adsorption / desorption energy, and q_{max} is the maximum sorption upon complete saturation of the substrate surface. (Adediran *et al.*, 2007) Therefore, Q_{max} represent the rate of adsorption and KL is the energy factor. The Q_{max} for different phytoestrogen i.e Formononetin, Genistein, Coumestrol, Daidzein and Biochanin A was 0.844, 0.836, 0.822, 0.799 and 0.305 $\mu\text{g/g}$, respectively.(Table 4.8(a)). This shows the adsorption of phytoestrogen by nanocrystalline zeolite NaX. The trend in adsorption was in the following order: Formononetin >Genistein >Coumestrol >Daidzein> Biochanin A (Table: 4.8(b)) which agreed with results of dynamic adsorption experiment. As adsorption Coefficient KL is related to the apparent energy of sorption. This could mean that the energy of adsorption is not very favorable for Biochanin A than the rest of the phytoestrogen as the KLvalue is high.

Table:4.8(a) Isothermal parameter of phytoestrogen on NaX zeolite.

Langmuir isotherm				
Adsorbate	Q_{max}	KL	R^2	R_L
Biochanin A	0.305	44.16	0.9977	0.053
Formononetin	0.844	32.11	0.9996	0.014
Coumestrol	0.822	36.7	0.9993	0.018
Genistein	0.836	40.16	0.9971	0.035
Daidzein	0.799	42.19	0.9995	0.037

Similarly, The adsorption (Q_{max}) values of Daidzein, Formononetin, Genistein, Coumestrol and Biochanin A was 11.990, 2.2381, 1.712, 0.8611 and 0.012 mg/g, respectively by nanocrystalline zeolite Beta. The KL value for Daidzein is lowest, indicating that it is better adsorbed by Beta zeolite.

Table:4.8 (b) Isothermal parameter of phytoestrogen on Beta zeolite.

Adsorbate	Langmuir isotherm			
	Q_{max}	KL	R^2	R_L
Biochanin A	0.012	30.87	0.9916	0.15
Formononetin	2.2381	2.266	0.9997	0.019
Coumestrol	0.8611	23.036	0.9921	0.26
Genistein	1.712	3.496	0.997	0.06
Daidzein	11.990	1.961	0.985	0.20

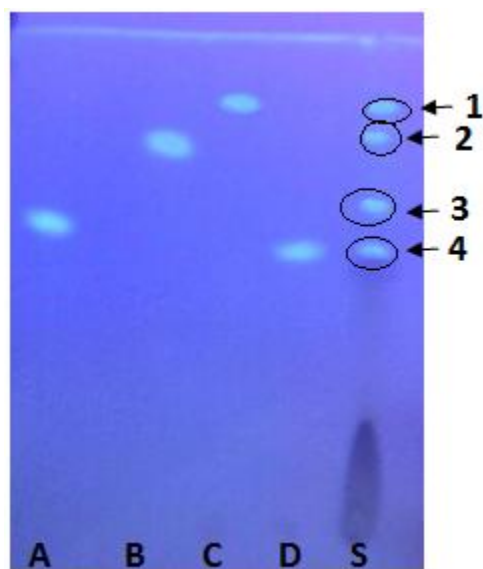
According to the above data, it was observed that Beta zeolite is better adsorbent compare to NaX as the Q_{max} values were high compare to NaX and values for energy of adsorption was low. Adsorption is an exothermic process with the heat released for physical adsorption. Heat of adsorption and entropy (size and configurational entropy) control the mixture adsorption selectivity in adsorption. These are represented by KL parameter. In case of NaX these values are high indicating that more energy is require for adsorption process.

The isotherm corrections can be measured using R_L value, R_L indicates the shape of isotherm. In the above analysis R_L value was $0 < R_L < 1$, which is refer to favorable isotherm (Table 4.8 (a) and (b)).

4.4 Detection of phytoestrogen in soy based industrial wastewater

4.4.1 Thin layer chromatography (TLC) analysis

Phytoestrogen standard solutions (as reference) and soy industrial waste water sample in methanol (0.5 μ g/ml) were used, and the development was carried out in a solvent system of chloroform/methanol (89: 11,v/v) on silica gel plates. Detection was carried out directly at UV-254 nm after exposure to fumes of concentrated ammonia solution. The analysis of TLC plate shows that sample contains different types of phytoestrogens as distinguished blue-white fluorescent spots were observed under U.V. illuminator (Fig: 4.10). R_f value of the spots calculated as under (Table 4.9).



Spots	Rf value (Sample)	Rf value (Standards)
1	0.59	0.60
2	0.56	0.55
3	0.45	0.46
4	0.42	0.40

Table 4.9. Rf value of different spots.

Fig: 4.10 TLC chromatograms of soy sample.

As the Rf value of spots corresponds to the known standard phytoestrogens i.e Biochanin A (C) (Rf=0.60), Formononetin (B) (Rf=0.55), Genistein (A) (Rf=0.46) and Daidzein (D) (Rf=0.40). Thus, this TLC analysis shows that the sample contained above mention phytoestrogens (Fig 4.7).

In TLC analysis separation of compounds is based on the competition of the solute and the mobile phase for binding places on the stationary phase. For instance, if normal phase silica gel is used as the stationary phase it can be considered polar. Given two compounds which differ in polarity, the more polar compound has a stronger interaction with the silica and is therefore more capable to dispel the mobile phase from the binding places. Consequently, the less polar compound moves higher up the plate (resulting in a higher Rf value). If the mobile phase is changed to a more polar solvent or mixture of solvents, it is more capable of dispelling solutes from the silica binding places and all compounds on the TLC plate will move higher up the plate.

4.4.2 Spectrophotometric detection of sample

The spots of phytoestrogens detected on Thin Layer Chromatographic plates, were scrapped out and the separated phytoestrogens were dissolved in methanol. The absorbance of individual phytoestrogen was measured at respective wavelength (Table:4.10).

Phytoestrogens	Absorbance at respective λ_{\max}	Concentration (ng/l)
Biochanin A	2.624 (236)	115
Formononetin	0.318(248)	150
Genistein	0.205(260)	294
Daidzein	0.510(232)	341

Table:4.10 Spectrophotometric analysis of sample.

4.4.3 High Performance Liquid Chromatography (HPLC) analysis of sample

Confirmation of presence of phytoestrogen was based on a comparison of retention time of phytoestrogen standard and unknown peaks in the sample. The retention time of Daidzein is 5.72 (Fig: 4.11). It was observed that retention time of standard and sample is approximately same.

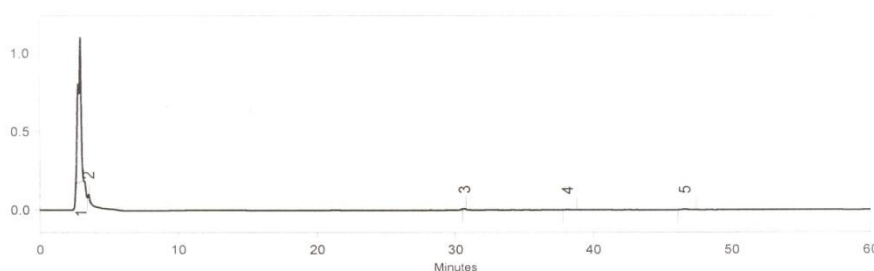


Fig:4.11 HPLC analysis of standard Daidzein

Above analysis confirmed that sample contained phytoestrogens. When sample was refluxed and analysed by HPLC, a single peak was identified at retention time of 5.675min with peak area of 97688057 (Table 4.11).

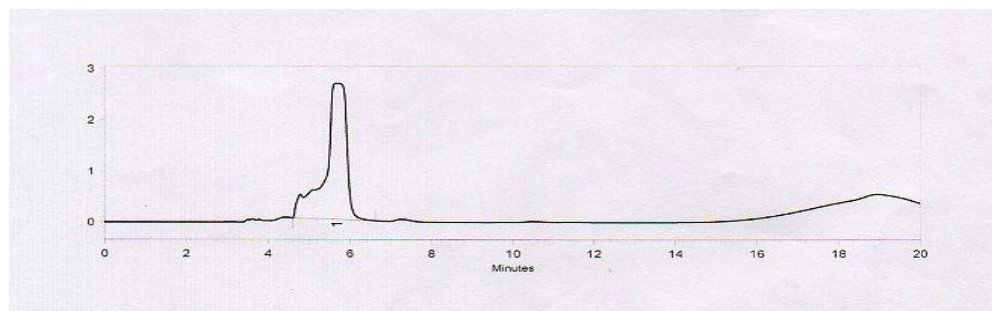
Peak	Retention Time	Peak Area	Area Percent
Sample	5.675	97688057	100
Treated Sample	5.692	37630417	100

Table 4.11 Retention time (min) and peak area.

After treatment with nanocrystalline zeolite Beta, the sample was again subjected to HPLC, reduction in Peak area was observed of 37630417.

The results show that the nanocrystalline zeolite Beta was effective in adsorption of phytoestrogens, which were present in sample (Fig: 4.12). The reduction percentage of phytoestrogen in sample using nanocrystalline zeolite Beta was 60%.

A



B

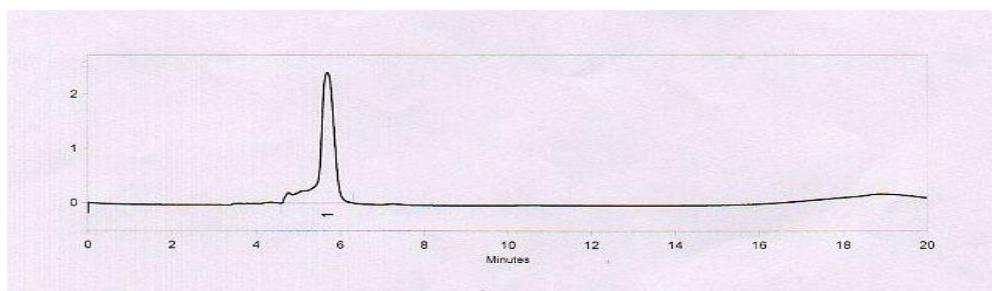


Fig: 4.12 Representative chromatogram of soy sample without (a) and with (b) treatment of nanocrystalline zeolite Beta.

SALIENT FINDINGS

1. The two FAU and BEA type nanozeolites were synthesized by changing the Si/Al ratio and characterized by XRD and SEM techniques, which confirmed their crystalline structure and particle size in nanometer range.
2. Synthesized nanocrystalline zeolites were used for further study of adsorption of phytoestrogen. The dosage of the adsorbent (nanocrystalline zeolites NaX and Beta) and time of contact for treatment of phytoestrogen was optimized.
3. 1µg/ml of phytoestrogens was treated with 1mg dose of adsorbent (nanocrystalline zeolite NaX and Beta) and maximum adsorption was analyzed at the range of 1-6 minutes. The comparative study of nanocrystalline NaX and Beta was performed for maximum adsorption of phytoestrogens.
4. The rate of adsorption and selectivity of particular phytoestrogen was studied using Langmuir Model. Beta-nano zeolite was found to be more effective and rate of adsorption was calculated as maximum in case of Daidezin.
5. The described results indicate that nanocrystalline zeolite Beta have interesting properties concerning the removal of phytoestrogens from water. The adsorption capacity of nanocrystalline zeolite NaX was less compared to nanocrystalline Beta, as the pore size of nanocrystalline beta was smaller compared to nanocrystalline NaX.
6. Phytoestrogens were detected in soy waste water sample using Thin Layer Chromatography technique and concentration of phytoestrogens was found as 900ng/l.
7. Overall, results confirmed that phytoestrogens have affinity for nanozeolite and it was observed that nanocrystalline Beta has potential for removal of phytoestrogen, as significant reduction (60%) was reported. This could represent a simple solution to the problem of cleaning up industrial wastewater at relatively low costs.

REFERENCES

- Adediran GO, Nwosu FO, Adekola FA (2007) Some Langmuir adsorption parameter of activated carbon produced from local materials, Nigeria J. Pure and Appl. Sci, 15, 1075-1082.
- Allen E, Doisy EA (1923) An ovarian hormone: preliminary report on its location, extraction and partial purification, and action in test animals, JAMA 81, 819-821.
- Anstead GM, Carlson KE, Katzenellenbogen JA (1997) The estradiol pharmacophore: ligand structure-estrogen receptor binding affinity relationships and a model for the receptor binding site, Steroids, 62, 268-303.
- Baerlocher C, Meier WM, Olson D H eds (2001) Atlas of Zeolite Framework Types, 5th revised ed., Elsevier Science, Amsterdam, 302 pp. frei herunterladbar von <http://www.zeolites.ethz.ch/Zeolites/PDFfiles.htm> Atlas online: <http://www.iza-structure.org>.
- Bagchi D, Das DK, Tosaki A, Bagchi M, Kothari SC (2001) Benefits of resveratrol in women's health, Drugs Exp Clin Res, XXVII, 233-248.
- Beck A B (1964) The oestrogenic isoflavones of subterranean clover, Aust. J. Agric. Res., 15, 223-230.
- Beekman ATF, Copeland JRM, Prince MJ (1999) Review of community prevalence of depression in later life, British Journal of Psychiatry, 174, 307-311.
- Bickoff EM, Booth AN, Lyman RL, Livingston AL, Thompson CR, DeEds F (1957) Coumestrol, a new estrogen isolated from forage crops, Science, 126, 969-970.
- Bowen TC, Noble RD, Falconer JL (2004). Fundamentals and applications of pervaporation through zeolite membranes, J. Membr. Sci., 245.
- Bowman RS (2003) Review: Applications of surfactant modified zeolites to environmental remediation, Microporous and Mesoporous Materials, 61, 43-56.
- Breck DW (1964) Zeolite Molecule Sieves, John Wiley, New York.

- Breck DW (1974) Zeolite molecular sieves, *Journal of Colloid and Interface Science*,305, 17–24.
- Chan RY, Chen WF, Dong A, Guo D, Wong MS (2002) Estrogen-like activity of ginsenoside Rg1 derived from *Panaxnotoginseng*, *J Clin Endocrinol Metab*, 87, 3691-3695.
- Charkhi A, Kazemian H, Kazemeini M (2010) Optimized experimental design for natural Clinoptilolite zeolite ball milling to produce nano powders, *Powder Technology*, doi: 10.1016/j.powtec.2010.05.034.
- Corma A (2003) *J. Catal*, 216, 298.
- Costello CH, Lynn EV (1950) Estrogenic substances from plants: I. Glycyrrhiza, *J Am Pharm Assoc* ,39, 177-180.
- Duke JA(1981) *Handbook of Legumes of World Economic Importance*, Plenum Press, New York.
- Fotsis T, Pepper M, Adlercreutz H (1993) Genistein, a dietary-derived inhibitor of in vitro angiogenesis, *Proc Natl Acad Sci USA*, 90, 2690-2694.
- Franke AA (1995) HPLC determination in biological fluids, *Proc. Soc. Exp. Biol. Med.* 208, 18.
- Franke AA, Custer LJ, Cerna CM, Narala KK (1994) Quantitation of phytoestrogens in legumes by HPLC, *J. Agric. Food Chem.*,42.
- Franke AA, Custer LJ, Wilkens LR (2002) Liquid chromatographic-photodiode array mass spectrometric analysis of dietary phytoestrogens from human urine and blood, *J Chromatogr B Analyt Technol Biomed Life Sci* ,777, 45-59.
- Giles CH, Smith D, Huitson A, *J. Colloid Interface Sci.*, 47, 755
- Gruber CJ, Tschugguel W, Schneeberger C, Huber JC (2002) Production and actions of estrogens, *N Engl J Med* , 346, 340-352.
- Higgins JB, LaPierre RB, Schlenker JL, Rohrman AC, Wood JD, Kerr GT, Rohrbaugh WJ (1988) The framework topology of zeolite beta, *Zeolites*,8, 446–452

- Hu JY, Aizawa T (2003) Quantitative structure-activity relationships for estrogen receptor binding affinity of phenolic chemicals, *Water Res*, 37, 1213-1222
- Ibarreta D, Daxenberger A, Meyer HHD (2001) Possible health impact of phytoestrogens and xenoestrogens in food, *APMIS*, 109, 161-184.
- Jacobs PA (1977) *Carboniogenic Activity of Zeolites*, Elsevier Sci. Pub. Co., New York.
- Kidd KA (2007) "Collapse of a Fish Population after Exposure to a Synthetic Estrogen," *Proceedings*.
- Kim SS, Shah J, Pinnavaia TJ (2003) *Chem. Mater*, 15, 1664
- Kingsbury JM (1964) *Poisonous Plants of the United States and Canada*, Prentice-Hall: Englewood Cliffs, NJ.
- Klabunde K J, Stark J, Koper O, Mohs C, Park DG, Decker S, Jang Y, Lagadic I, Zhang D (1996) *Phys. Chem.*, 100, 12142.
- Koningsveld H, Bennett JM (1999), *Mol. Sieves*, 2, 1.
- Kurzer MS, Xu X (1997) Dietary phytoestrogens, *Annu Rev Nutr*, 17, 353-381.
- Liggins J, Bluck LJC, Runswick S, Atkinson C, Coward WA, Bingham SA (2000) Daidzein and genistein content of fruit and nuts, *J. Nutr. Biochem*, 11, 326-331.
- Lookhart GL (1980) Analysis of coumestrol, a plant estrogen, in animal feeds by high performance liquid chromatography, *J Agric Food Chem*, 28, 666-667.
- Lundgren MS, Novak PJ (2009) "Quantification of Phytoestrogens in Industrial Waste Streams," *Environmental Toxicology and Chemistry*, 28, 2318-2323.
- Mahdi F, Abdolreza A (2011) Department of Chemical Engineering, Amirkabir University of Technology (Tehran Polytechnic) Tehran, Iran Food Process Engineering and Biotechnology Research Center, Amirkabir University of Technology (Tehran Polytechnic) Tehran, Iran.

Merken HM, Beecher GR (2000) Measurement of food flavonoids by high-performance liquid chromatography: A review, *Journal of Agricultural and Food Chemistry*, 48, 577-599.

Mintova S, Oison NH, Valchav V, Bein T (1999) *Science*, 283, 958
Modhera B, Chakraborty M, Parikh PA, Jasra RV (2008). Chemical Engineering Department, S.V. National Institute of Technology, Surat 395 007, India. Discipline of Inorganic Materials and Catalysis, Central Salt and Marine Chemical Research Institute (CSMCRI), Bhavnagar 364 002, India.

Mosselman S, Polman J, Dijkema R (1996) ER β : identification and characterization of a novel human estrogen receptor, *FEBS Lett*, 392, 49-53.

Naftolin F, Stanbury MG (2002) Phytoestrogens: are they really estrogen mimics, *Fertil Steril*, 77, 15-17.

Pratt DE, Birac PM (1964) Source of antioxidant activity of soybeans and soy products, *Journal of Food Science*, 44, 1720-1722.

Ravishankar R, Kirschhock C, Schoeman BJ, Vanoppen P, Grobet PJ, Storck S, Maier WF, Martens JA, Schryver FC, Jacobs PA (1998) *Phys. Chem.B*, 102, 2633.

Ruthven DM (1988) Zeolites as Selective Adsorbents, *Chemical Engineering Progress*, 42-50.

Santi R, Makela S, Strauss L, Korkman J, Kostian ML (1998) Phytoestrogens: potential endocrine disruptors in males, *Toxicol Ind Health* 14, 223-237.

Schoeman BJ, Sterte J, Otterstedt J (1994). *Zeolites*, 14, 110.

Setchell KDR (1998) Phytoestrogens: the biochemistry, physiology, and implications for human health of soy isoflavones, *Am J Clin Nutr*, 68, 1333S-1146S.

Tamer, N H (2006) M.Sc., Department of Chemical Engineering, Supervisor: Prof. Dr. Hayrettin Yucel Co-Supervisor: Prof. Dr. Nurcan Bac, 80 pages

Tosheva L, Valchev VP (2005) *Chem. Mater.*, 17, 2494.

References

Turk A (1997) Adsorption In Engineering Control of Air Pollution: Air Pollution, Volume IV, Stern, AC, Ed.; New York: Academic Press.

Verduijn JP (1993) Patent No. WO9308125.

Bragg WL (1913) Proc. Cambridge Phil. Soc. 17, 43.

Wang CC, Prasain JK, Barnes S (2002) Review of the methods used in the determination of phytoestrogens, J Chromatogr B Analyt Technol Biomed Life Sci, 777, 3-28.

Weber TW, Chakkravorti R K (1974) Pore and solid diffusion models for fixed-bed adsorbers, AIChE Journal, 20, 228–238.